THE ROLE OF THE PIP5 KINASE GAMMA 87 ISOFORM IN THE REGULATION OF THE ACTIN CYTOSKELETON

APPROVED BY SUPERVISORY COMMITTEE

Helen L. Yin, Ph.D. (mentor)

Michael G. Roth, Ph.D. (chair)

Joseph P. Albanesi, Ph.D.

Michael K. Rosen, Ph.D.

DEDICATION

I would like to dedicate this dissertation to my family, Dan, Melodee, Danny, Timmy, and Stephen Corgan, for their continuing love and support.

THE ROLE OF THE PIP5 KINASE GAMMA 87 ISOFORM IN THE REGULATION OF THE ACTIN CYTOSKELETON

by

ANNE MARIE CORGAN

DISSERTATION

Presented to the Faculty of the Graduate School of Biomedical Sciences

The University of Texas Southwestern Medical Center at Dallas

In Partial Fulfillment of the Requirements

For the Degree of

DOCTOR OF PHILOSOPHY

The University of Texas Southwestern Medical Center at Dallas

Dallas, Texas

October 2009

ACKNOWLEDGEMENTS

I would like to thank the members of my Graduate Committee, particularly my mentor, Dr. Helen Yin, and all of the members of the Yin lab. I would also like to thank all of my friends here in Dallas who have made graduate school such an unforgettable experience.

THE ROLE OF THE PIP5 KINASE GAMMA 87 ISOFORM IN THE REGULATION OF THE ACTIN CYTOSKELETON

Anne Marie Corgan Ph.D.

The University of Texas Southwestern Medical Center at Dallas, 2009

Supervising Professor: Helen L. Yin, Ph.D.

Abstract: Phosphatidylinositol-4,5-bisphosphate (PIP2) is an important regulator of the actin cytoskeleton and plasma membrane functions. It is primarily synthesized by the type 1 phosphatidylinositol 4 phosphate 5 kinases (PIP5Ks). Mammals have three PIP5K genes (*PIP5Kα, PIP5Kβ,* and *PIP5Kγ*), and the γ isoform has two ubiquitous 90 kDa and an 87 kDa splice variants. We found that the depletion of each PIP5K isoform individually by RNA interference (RNAi) or gene knockout by homologous recombination generated distinct changes in the actin cytoskeleton and signaling responses. The actin phenotype of the PIP5Kγ

depletion (using pan siRNA, which is directed against a common sequence shared by the 90 and 87kDa isoforms) in HeLa cells is particularly striking: it results in increased actin stress fibers, decreased chemotaxis, and increased adhesion to fibronectin-coated substrates. There is also a striking increase in prominent focal adhesions (FA). Using real-time IRM, we found that the turnover of FA is 48% slower in the PIP5Kγ depleted cells. Likewise, there is a large decrease in the dynamic turnover of green fluorescent protein (GFP)-labeled vinculin and paxillin in FA, as monitored by fluorescence recovery after photobleaching. Since PIP5Kγ90 has already been implicated in FA assembly, we depleted it specifically without depletion of the much more abundant PIP5Kγ87 by using a PIP5Kγ90 specific targeting sequence not found in PIP5Kγ87. This fails to produce robust stress fibers. Overexpression of PIP5Kγ87, but not the kinase dead enzyme, is able to rescue the pan PIP5Kγ knockdown actin phenotype in HeLa cells. Thus, PIP5Kγ87 is the major contributor to the pan PIP5Kγ depletion/knockout robust actin and FA phenotype. Similar results were obtained in mouse embryonic fibroblasts (MEFs) from *PIP5Kγ-/-* mice. We sought to identify the molecular mechanisms of the PIP5Kγ depleted actin phenotype. Inhibitors of myosin, Rho-associated coiled-coil-containing protein kinase (ROCK), and RhoA GTPase all decreased the amount of thick actin stress fibers in PIP5Kγ RNAi cells, suggesting that the phenotype is due to abnormal RhoA activation. This is

confirmed by the finding that RhoA activity is elevated in PIP5Kγ depleted/knock out cells. We hypothesize that PIP5Kγ regulates the actin cytoskeleton by inhibiting Rho, and thus its downstream effectors ROCK and myosin.

TABLE OF CONTENTS

PRIOR PUBLICATIONS

Fraley, T.S., T.C. Tran, **A.M. Corgan**, C.A. Nash, J. Hao, D.R. Critchley, and J.A. Greenwood. (2003) Phosphoinositide binding inhibits α-actinin bundling activity. *J. Biol. Chem.* 278: 24039-24045.

Corgan, A.M., C.A. Singleton, C.B. Santoso, and J.A. Greenwood. (2004) Phosphoinositides differentially regulate α-actinin flexibility and function. *Biochem. J.* 378: 1067-1072.

LIST OF FIGURES

LIST OF TABLES

LIST OF ABBREVIATIONS

ACAP1	Arf-GAP with coiled-coil, ANK repeat and PH domain protein 1
ARF6	ADP-ribosylation factor 6
FA	focal adhesion
F-actin	filamentous actin
FRAP	flourescene recovery after photobleaching
GFP	green fluorescent protein
IRM	interference reflection microscopy
KD	kinase dead
MEF	mouse embryonic fibroblast
PI(4)P	phosphatidylinositol 4-phosphate
PIP_2	phosphatidylinositol-4,5-bisphosphate
PIP5K	type I phosphatidylinositol 4 phosphate 5 kinase
PLD2	phospholipase D2
ROCK	Rho-associated coiled-coil-containing protein kinase
siRNA	small interfering RNA
WT	wild type

CHAPTER 1: INTRODUCTION

I. PIP5 Kinases Isoforms

The primary route of PIP_2 synthesis is through the phosphorylation of phosphatidylinositol 4-phosphate (PI(4)P) by the type I phosphatidylinositol 4 phosphate 5 kinases (PIP5Ks) (Stephens et al., 1991, Whiteford et al., 1997, Doughman et al., 2003a). Mammals have three PIP5K genes: *PIP5Kα*, *PIP5Kβ*, and *PIP5Kγ* (Ishihara et al., 1996, Ishihara et al., 1998, Loijens et al., 1996). These lipid kinases contain a highly conserved central catalytic domain of approximately 400 residues and have non-conserved amino and carboxyl terminal sequences (Fig. 1). There is increasing evidence that these isoforms have unique and non-redundant roles, presumably due to the production of discrete pools of PIP_2 at distinct locations.

PIP5Kα

PIP5Kα -/- mice have a platelet aggregation defect and are less fertile than wild type mice (Wang et al., 2008). Boronenkov et al. (1998) found that PIP5Kα localizes to the nucleus where it co-localizes with nuclear speckles. PIP5Kα induces membrane ruffles in a Rac dependent manner (Doughman et al., 2003b), after recruitment to the plasma membrane by Ajuba (Kisseleva et al., 2005). PIP5Kα has been shown to interact with β-arrestin2 upon activation of the β2-adrenergic receptor (Nelson et al., 2008) and is also required for actin polymerization during the ingestion phase of Fcγ receptor mediated phagocytosis (Coppolino et al., 2002, Mao et al., 2009).

PIP5Kβ

PIP5Kβ -/- mice have no striking abnormalities as compared to wild type mice, but do display an increased Ca^{2+} response and reduced levels of cortical actin filaments (F-actin) (Sasaki et al., 2005). Additionally, PIP_2 produced by PIP5Kβ is important for the regulation of clathrin-mediated endocytosis (Padron et al., 2003), phospholipase D2 (PLD2) activity (Divecha et al., 2000), oxidative stress induced apoptosis, and cytoskeletal remodeling (Halstead et al., 2006 and Chen et al., 2009).

PIP5Kγ

In humans, it has been reported that a missense mutation that causes a mutation within the catalytic domain of PIP5Kγ results in lethal contractural syndrome (Narkis et al., 2007). This pheonotype is not replicated in either of the two independently generated mouse *PIP5Kγ -/-* lines that have been created. One of them (generated by the Abrams lab) results in *PIP5Kγ -/-* mice which display embryonic lethality at E11.5 and which by day E9.5 are smaller and have cardiovascular defects, which appear to be the cause of death (Wang et al., 2007). In the other line (generated by the De Camelli lab), *PIP5Kγ -/-* mice die within 24 hours of birth, possible due to significant neuronal defects that result in an inability to eat (Di Paolo et al., 2004). PIP5Kγ has two major splice variants, PIP5Kγ87 and PIP5Kγ90 (Ishihara et al., 1998). A third isoform, PIP5Kγ93, has been identified that is only expressed in the brain (Giudici et al., 2004). PIP5Kγ87 synthesizes the pool of PIP_2 involved in G protein coupled receptor mediated production of IP_3 in HeLa and mast cells (Wang et al., 2004, Vasudevan et al., 2009) and it has been implicated in regulating actin dynamics to promote clustering of Fcγ receptors during the attachment phase of phagocytosis (Mao et al., 2009). PIP5Kγ90, which is enriched in FAs, has an important function in FA assembly (Di Paolo et al., Ling et al., 2002) and in synaptic vesicle endocytosis

(Nakano-Kobayashi et al., 2007, Morgan et al., 2004). Our studies will focus on the role of PIP5Kγ in the regulation of the actin cytoskeleton and FA disassembly.

II. PIP5Kγ Binding Partners

Talin

The FERM domain of talin binds to the unique c-terminus of PIP5Kγ90 and stimulates the kinase activity of PIP5Kγ90 (Di Paolo et al., 2005, Ling et al., 2002). This interaction is regulated by the phosphorylation of PIP5Kγ tyrosine 644 by Src and dephosphorylation of serine 650 by Shp-1 (Ling et al., 2003, Lee et al., 2005, Bairstow et al., 2005, De Pereda et al., 2005, Kong et al., 2006). HeLa cells depleted of PIP5Kγ90 and stimulated with EGF have been shown to have fewer talin containing adhesions and decreased rates of talin assembly to adhesions as compared to cells treated with control siRNA (Sun et al., 2007).

PLCγ

PLCγ binds to PIP5Kγ in HeLa cells and EGF stimulation blocks this interaction (Sun et al., 2007). Recent evidence suggests that PIP5Kγ synthesizes a distinct PIP_2 pool that is hydrolyzed by PLCγ to regulate the release of calcium ions from ER stores (Vasudevan et al., 2009).

E- and N-cadherins

In A431 epithelial cells, PIP5Kγ87 was found to be recruited to the intracellular junction where it co-localized with E-cadherin (Akiyama et al., 2005). E-cadherin was later found to directly interact with PIP5Kγ (Ling et al., 2007), and N-cadherin has also been shown to associate with PIP5Kγ (Sayegh et al., 2007).

Clathrin Adaptor Proteins

All PIP5 Kinases have been reported to weakly interact with the μ2 subunit of the clathrin adaptor protein complex AP-2 via their kinase core domain (Krauss et al., 2006). PIP5Kγ90, but not PIP5Kγ87, strongly interacts with the μ subunit of AP1B (Ling et al., 2007), with the β2 subunit of AP-2 (Nakano-Kobayashi et al., 2007, Thieman et al., 2009), and with the μ2 subunit of AP2 (Bairstow et al., 2006).

Rho Family GTPases

RhoA is known to physically associate with the PIP5Ks (Ren et al., 1996, Oude Weernink et al., 2004). The activity of PIP5Ks in lysates from mouse fibroblasts and HEK-293 cells has been shown to be increased in the presence of activated RhoA (Chong et al., 1994, Oude Weernink et al., 2000). RhoA and ROCK have been found to regulate the activity of PIP5Ks in HEK-293 cells (Oude Weernink et al, 2000, Oude Weernink et al., 2004). Rac1 has also been shown to directly interact with and activate PIP5Kγ in a RhoA independent manner (Tolias et al., 1995, Oude Weernink et al., 2004). Recently, Mao et al. (2009) found new evidence that, in addition to its role as a downstream effector of RhoA and Rac, PIP5Kγ also acts upstream by increasing Rac and inhibiting RhoA activity.

ARF6

ADP-ribosylation factor 6 (ARF6) interacts with and stimulates the kinase activity of PIP5γ (Aikawa *et al.*, 2003, Krauss *et al.*, 2003). Overexpression of ARF6Q67L, a constitutively active mutant, causes the translocation of PIP5Kγ from the plasma membrane to endosomal membranes in PC12 cells (Aikawa *et al.*, 2003).

III. Effects of PIP5Kγ on Cell Motility and Regulation of the Actin Cytoskeleton

Adhesion and Migration

When overexpressed, both PIP5Kγ87 and PIP5Kγ90 target to the plasma membrane, but unlike PIP5Kγ87, PIP5Kγ90 also localizes to FAs (Di Paolo et al., 2002, Ling et al., 2002). High level PIP5Kγ90 overexpression in NIH 3T3 leads to a disruption of FAs (Di Paolo et al., 2002). PIP5Kγ87, but not PIP5Kγ90, has been reported to play a role in PLD2 stimulated adhesion through increased integrin β_1 and β_2 binding to their substrates (Powner et al., 2005). Both PIP5Kγ87 and γ90 have been identified as components of the uropod in primary neutrophils (Lokuta et al., 2007). Overexpression of a PIP5Kγ90 kinase dead mutant in neutrophil-like HL-60 cells inhibited detachment of the trailing edge (Lokuta et al., 2007). Neuronal cells from *PIP5Kγ -/-* mice have decreased cell migration through filters in a transwell assay compared to *PIP5Kγ +/+* cells (Wang et al., 2007). Sun et al. (2007) found that upon depletion of PIP5Kγ90 in HeLa cells, there is decreased migration towards an EGF gradient. This defect could be rescued by stably expressed wild type PIP5Kγ90, but not by a kinase dead mutant, a mutant unable to bind to talin, or PIP5Kγ87. Cells depleted of only the PIP5Kγ90 isoform also showed decreased motility towards a hepatocyte growth factor gradient, but migration towards an LPA or SDF1α gradient was unaffected.

Actin

It has long been apparent that the PIP5 kinases have a role in the regulation of the actin cytoskeleton. Overexpression of any of the three PIP5K isoforms leads to the formation of actin comets (Rozelle et al., 2000, Padron et al., 2003). Recent evidence suggests that PIP5Kγ90 is essential for association of the cytoskeleton

with the plasma membrane (Wang et al., 2008a) and PIP5Kγ has a reported role in the formation of adherens junctions (Ling et al., 2007). Cytoskeletal effects of PIP5Kγ knock out have been somewhat more contradictory. In cardiocytes from embryonic *PIP5Kγ-/-* mice, Wang et al. (2007) observed a cytoskeletal defect. Sarcomeres had disorganized actin which did not associate with fascia adherens. Mao et al. (2009) found that *PIP5Kγ-/-* bone marrow macrophages (from the De Camilli line) have more F-actin and a more elongated shape. However, in megakaryocytes derived from the Abrams *PIP5Kγ-/-* mouse line, there is no detectable change in F-actin levels (Wang et al., 2008a). We will focus on further elucidating the actin phenotype PIP5Kγ depleted HeLa cells and *PIP5Kγ-/-* MEF cells from the De Camili line.

IV. The Role of PIP2 in Focal Adhesions

FAs are sites of attachment of the cell to the extracellular matrix via integrins. FAs mediate inside-out and outside-in signaling, and are therefore able to sense and respond to the extra-cellular environment to regulate cell growth, differentiation, adhesion, and migration (Hynes et al., 1992, Schwartz et al., 1995, Hynes 1999, Liddington et al., 2002). Recently, sixty-six molecules have been reported to be peripherally associated with FAs and another ninety have been identified that can be directly localized to FAs (Zaidel-Bar et al., 2007). These including the PIP_2 regulated cytoskeletal proteins vinculin, talin, and α-actinin (Zaidel-Bar et al., 2007). Winograd-Katz et al. (2009) recently completed a large scale screen which investigated the effects of depleting individual FA proteins by RNAi on cell shape, FA morphology, distribution and cell coverage. This approach identified many more proteins that influence FA behavior.

Vinculin

Vinculin has long been implicated in the regulation of cell motility and FAs. In 1992, overexpression of vinculin in 3T3 cells was shown to negatively affect cell motility (Fernandez et al, 1992). Soon thereafter, it was shown that depletion of vinculin in 3T3 cells by siRNA had an opposite effect on cell motility, i.e. quicker wound closure than control cells, and that this was coupled with a reduced amount of spreading and smaller FAs (Fernandez et al., 1993). *Vinculin -/-* F9 embryonal carcinoma cells are reported to have decreased spreading and adhesion and increased motility (Coll et al., 1995). The migratory effects could be rescued by overexpression of wild type (WT) vinculin (Xu et al., 1998). Similarly, *vinculin -/-* MEFs display decreased adhesion and increased migration (Xu et al., 1998a). In agreement with these results, *vinculin -/-* immortalized MEFs have been shown to have greater cell motility, as measured by a wound closure assay, spread less and at a slower rate, and have smaller FAs that turnover faster than those of *vinculin +/+* MEFs (Saunders et al. 2006).

Interactions between the head and tail of vinculin obstruct the binding sites of other proteins resulting in auto-inhibition (Bakolitsa et al., 2004, Borgon et al., 2004). Chen et al. (2005) demonstrated that vinculin in the cytosol is in an auto-inhibited state and vinculin in FAs primarily exists in the active state. Overexpression of either the head or tail domain of vinculin alone in *vinculin -/-* F9 embryonic carcinoma cells enhanced migratory effects, suggesting a role for vinculin in repressing cell motility that is dependent upon the auto-inhibitory interactions between the head and tail domains (Xu et al., 1998b).

Vinculin interacts with PIP_2 and its two PIP_2 binding sites have been mapped by X-ray crystallography to a basic region on helix 3 and a basic collar at the c-terminus of vinculin (Bakolitsa et al., 1999, Bakolitsa et al, 2004). Binding of PIP_2 to vinculin is sufficient to release the auto-inhibition of vinculin (Weekes et

al., 1996, Gilman et al., 1996, Huttelmaier et al., 1998). Overexpression of a vinculin mutant, which is recruited to FA but is unable to bind to PIP_2, in *vinculin -/-* MEFs was unable to rescue motility and spreading defects and resulted in increased FA stability, as measured by interference reflection microscopy (IRM) (Saunders et al. 2006). These results suggest the importance of the PIP_2 and vinculin interaction in the disassembly of FAs. They also corroborated an earlier report of the effects of overexpression of a WT and mutant vinculin in B16-FA mouse melanoma cells (Chandrasekar et al., 2005). In these cells, overexpression of the vinculin mutant that was unable to bind lipids resulted in defective cell spreading, cell motility, and five times lower overall adhesion turnerover rates (Chandrasekar et al., 2005).

Talin

Talin is an important component of FAs. It binds to β integrin, resulting in activation of the integrin (Tadokoro et al., 2003, Wegener et al., 2007). The interation between the talin head domain and tail domain masks the β integrin binding site, but binding of PIP_2 to the talin head domain relieves this auto-inhibition and facilitates binding between talin and integrin (Martel et al., 2001, Goksoy et al., 2008).

There are two talin isoforms. *Talin 1 -/-* embryonic stem cells are defective in cell spreading and fail to form actin stress fibers and FAs (Priddle et al., 1998). However, differentiated *talin -/-* embryonic strem cells are able to form FAs and stress fibers (Priddle et al., 1998), possibly due to compensatory effects of talin 2 (Monkley et al., 2001). Indeed, when *talin -/-* fibroblasts were depleted of talin 2 by siRNA, the cells displayed a loss of FAs and an impairment of sustained cell adhesion and spreading (Zhang et al., 2008).

α-actinin

α-actinin serves to bind and bundle actin into stress fibers and to link the actin cytoskeleton to integrin (Otey et al., 1990, Pavalko et al., 1991). PIP_2 has been shown to interact with the calponin homology 2 domain of α-actinin (Fukami et al., 1996, Fraley et al., 2003). When PIP_2 is bound to α-actinin, it inhibits the ability of α-actinin to bind and bundle actin (Fraley et al., 2003). Fraley et al. (2003) created an α-actinin mutant that has dramatically reduced binding to phosphoinositides. Later, using flourescence recovery after photobleaching (FRAP), Fraley et al. (2005) demonstrated that the turnover rate of this α-actinin mutant in FAs is 1.5 times slower than WT α-actinin in rat embryonic fibroblasts. Pre-incubation of α-actinin with PIP_2 protects against proteolysis by chymotrypsin *in vitro* (Corgan et al., 2004) and recently, it has been shown that binding of PIP_2 to α-actinin protects α-actinin from proteolysis by calpain 1 (Sprague et al., 2008).

PIP5K Isoforms

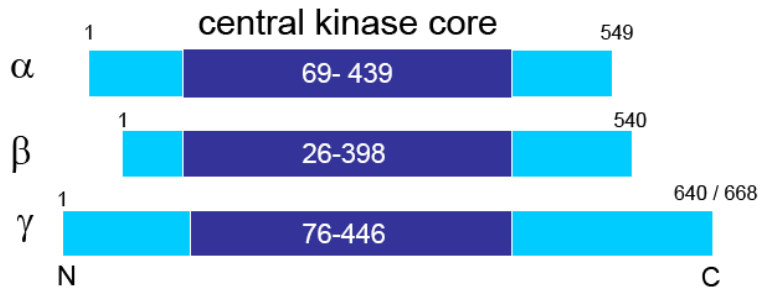

Figure 1. (Adapted, with permission, from Mao and Yin 2007.) PIP5Kα, PIP5Kβ, and PIP5Kγ have highly conserved central catalytic domains and non-conserved amino and carboxyl terminal sequences.

Focal Adhesions

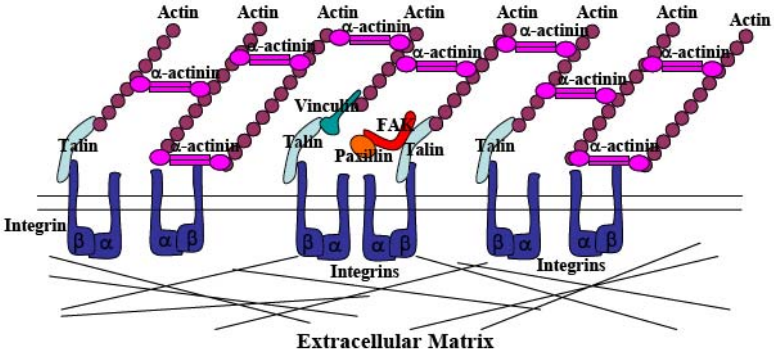

Figure 2. A simplified model of a FA. PIP_2 regulated proteins talin, vinculin, and α-actinin serve to connect the actin cytoskeleton to the cytoplasmic domain of β integrin which exists as a heterodimer with α integrin. Paxillin is also enriched at FAs.

CHAPTER 2: THE UNIQUE CYTOSKELETAL PHENOTYPE ASSOCIATED WITH THE DECREASE IN PIP5K GAMMA EXPRESSION

I. Loss of PIP5Kγ Results in a Distinct Actin Phenotype

Upon depletion of individual PIP5K isoforms in HeLa cells by siRNA (Padron et al., 2003), Ying Jie Wang, a former postdoctoral fellow in the Yin lab, found that there are isoform specific actin phenotypes. Depletion of PIP5Kα results in a rounder cell with a ring of actin, depletion of PIP5Kβ leads to a smaller cell with less actin, and cells depleted of PIP5Kγ have very robust stress fibers (Fig. 3A). The dramatic effect of PIP5Kγ depletion, with the marked increase in actin stress fibers, led me to focus my studies on the phenotype and mechanisms associated with the loss of PIP5Kγ.

To explore PIP5Kγ isoform specific effects upon the actin cytoskeleton, I first repeated Ying Jie Wang's work and treated HeLa cells with siRNA to PIP5Kγ and then confirmed the efficacy of the depletion via a Western blot (Fig. 3B). Cells depleted of PIP5Kγ have a distinct actin phenotype as visualized with immunofluorescence. These cells have very robust actin stress fibers and generally have a more elongated shape (Fig. 3C).

To further validate our findings of the striking actin phenotype in HeLa cells depleted of PIP5Kγ by RNAi, we next utilized MEF cells from *PIP5Kγ-/-* mice generated by the De Camilli lab (Di Paolo et al., 2004) to determine if they exhibit a similar phenotype. In initial studies examining the actin cytoskeleton

through the use of immunofluorescence, Xiaohui Zhu, a research assistant in the Yin lab, found the actin phenotype of *PIP5Kγ -/-* MEFs to be consistent with that of PIP5Kγ depleted cells. *PIP5Kγ -/-* MEFs had more robust actin stress fibers than the *PIP5Kγ +/+* cells (Fig. 3D).

The salient actin cytoskeletal phenotype of PIP5Kγ depleted cells based on immunoflourescence microscopy was corroborated biochemically by fluorometric F-actin quantitation in cell extracts. I verified that the PIP5Kγ depleted cells do indeed contain more filamentous actin than control cells (Fig. 4A). Likewise, *PIP5Kγ -/-* MEFs have more F-actin than *PIP5Kγ +/+* MEFs, recapitulating the RNAi phenotypes of HeLa cells (Fig. 4B).

Next, I sought to establish if there was an increase in FAs associated with these abundant stress fibers. Cells were treated with antibodies against the FA components paxillin and vinculin and the resulting confocal images allowed me to visualize the FAs present at the tips of the thick stress fibers. In comparing the FAs of the control and the PIP5Kγ depleted cells, a marked difference can be seen (Fig. 5). In parallel with the increase in actin stress fibers, FAs in PIP5Kγ depleted cells are more prominent than in control cells; they appear to be larger and more numerous.

II. Chemotactic Motility and Adhesion Phenotype

Since depletion of PIP5Kγ stabilizes FAs and actin stress fibers, we next examined the effects upon the motility of these cells. Ying Jie Wang subjected cells depleted of individual PIP5K isoforms to a transwell chemotactic motility assay. PIP5Kγ depleted cells migrate towards the chemotactic source much slower than control cells or cells depleted of other PIP5K isoforms (Fig. 6A),

suggesting that PIP5Kγ is particularly important for chemotaxis. This is in agreement with previous reports that depletion of either PIP5Kγ90 or both PIP5Kγ isoforms in HeLa cells results in a negative effect on cell migration towards an EGF gradient (Sun et al, 2007). Our subsequent line of investigation focused on the effects upon cell motility in *PIP5Kγ -/-* MEFs. In a wound healing assay, where confluent MEF monolayers were wounded with a scratch and the width of the wound was observed, *PIP5Kγ +/+* MEFs closed the wound completely after 8 hours, whereas *PIP5Kγ -/-* MEFs did not (Fig. 6B). Moreover, when the MEF cells were subjected to a transwell assay measuring chemotactic migration towards serum, we found that fewer *PIP5Kγ-/-* MEF cells migrated through the filter (Fig. 6C), upholding the RNAi phenotype in HeLa cells.

There have been conflicting reports on the roles of PIP5Kγ on cell adhesion. Previously, it has been reported that upon depletion of PIP5Kγ in MDCK cells by RNAi, the cells lost plasma membrane associated E-cadherin which was accompanied by an increase in cell spreading (Ling et al., 2007). In *PIP5Kγ -/-* megakaryocytes, the cells are reported to spread to the same extent as *PIP5Kγ +/+* cells and to extend lamellipodia normally (Wang et al., 2008). However, they generate abnormal plasma membrane blebs (Wang et al, 2008). Additionally, NIH 3T3 cells overexpressing PIP5Kγ87 showed a very slight decrease in cell spreading (Di Paolo et al., 2005).

I further characterized the phenotype of PIP5Kγ deficient HeLa cells on two facets of cell adhesion: attachment and spreading on fibronectin coated surfaces. At a concentration of 0.5 μg/ml of fibronectin, the PIP5Kγ depleted cells had spread to a significantly greater extent than the control cells (Fig. 7A). Differences in cell adhesion were corroborated by the results of a cell attachment

assay, in which the quantity of control and PIP5Kγ depleted cells attached to various concentrations of immobilized fibronectin were quantitated through a colormetric assay (Fig. 7B). We conclude that loss of PIP5Kγ in HeLa cells results in enhanced cell adhesion on fibronectin coated surfaces.

III. PIP5Kγ depleted cells display altered focal adhesion dynamics

Thus far, we have shown that PIP5Kγ depleted cells have a distinct phenotype consisting of abundant actin stress fibers and FAs, decreased chemotactic motility, and stronger adhesion to fibronectin. I next investigated if this phenotype is associated with aberrant FA dynamics. I used live cell imaging approaches to examine FA dynamics quantitatively. First, I used a FRAP assay, as described by Chandrasekar et al. (2005), to examine the turnover rates of two GFP-tagged FA components: vinculin and paxillin. Control or PIP5Kγ depleted HeLa cells were transfected with GFP-labeled paxillin or GFP-labeled vinculin. Individual FAs were photobleached and images were taken every 4 seconds for about 4 min. Fig. 8A follows the fate of GFP-paxillin in a single FA in a control cell and another in a PIP5Kγ depleted cell. The red arrows indicate the bleached region. Comparing the top and bottom panels at the 50 and 100 sec. time points, it's clear that the FA in the control cell is recovering much quicker than that in the PIP5Kγ depleted cell. I collected the intensity of the bleached region at each time point and fit the resultant data with a one phase exponential association curve, as exemplified in Fig. 8B, which provided us with the t1/2 and % recovery. Results from the FRAP experiments reveal that the PIP5KIγ depleted cells have about a 2-fold longer half-time of fluorescence recovery than control cells for both GFP-vinculin and GFP-paxillin (Table 1).

Next, I monitored the rate of FA turnover by live cell imaging using IRM, as described by Saunders et al. (2006). In this method, cells were imaged by time lapse for 60 min. The left upper panels of Fig. 9A depict the first and last time points of a typical experiment. The dark regions at the bottom of the cells are FAs. Individual images were filtered and thresholded to display only the dark FAs as appears in the lower left panels of Fig. 9A. In order to analyze these images, FA images from each time point were overlayed into a pseudocolor greyscale. Dark areas within this pseudocolor grayscale are indicative of a FA with very little variablitiy that has stayed static throughout most of the time points. Conversely, areas in the pseudocolor grey scale that are very light are indicative of a more dynamic FA; one that has only been present throughout some of the time points. The ratio of light grey pixels to dark grey pixels can be expressed as a FA turnover index (Saunders et al., 2006). PIP5Kγ depleted cells have a FA turnover index of 4.6 as opposed to the control cell FA turnover index of 2.2 (Fig. 9B, right panels). Thus, the FAs in PIP5Kγ depleted cells turn over 48% slower on average than those in control cells.

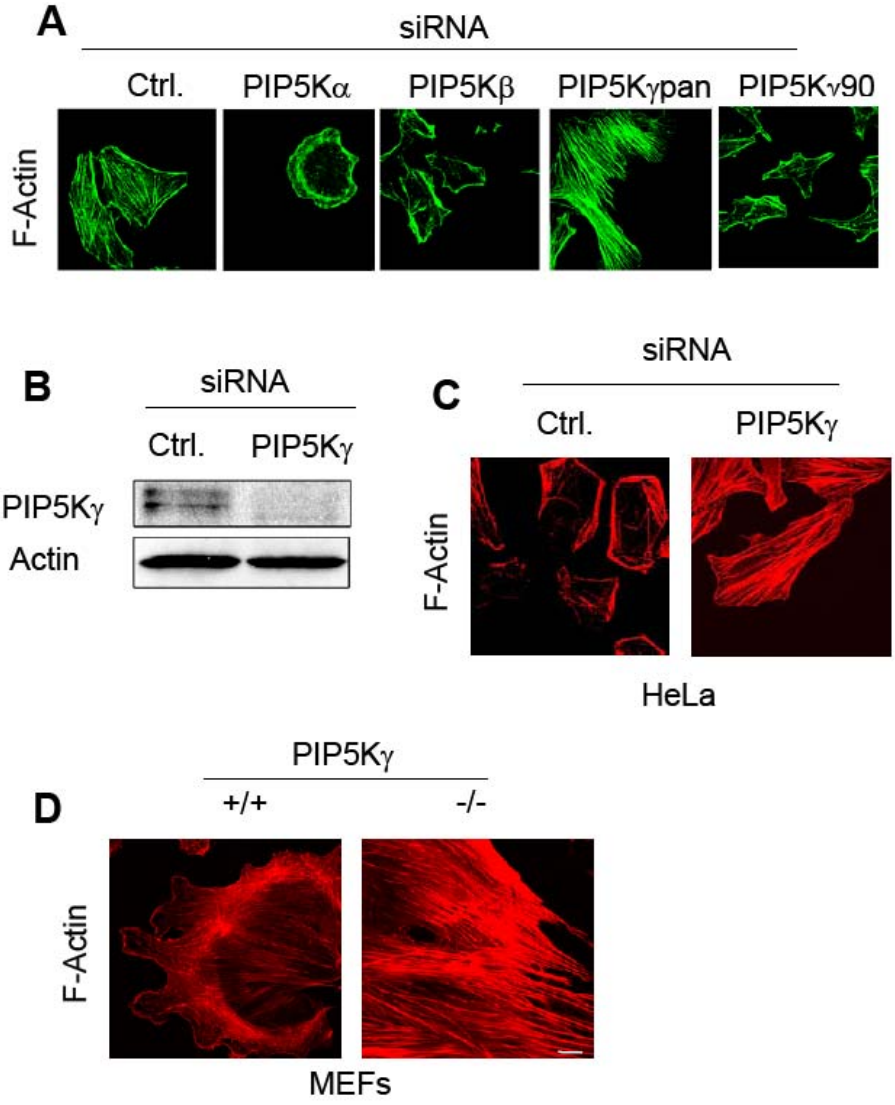
A
siRNA
Ctrl.
PIP5Kα
PIP5Kβ
PIP5Kγpan
PIP5Kγ90
F-Actin
B
siRNA
Ctrl.
PIP5Kγ
PIP5Kγ
Actin
C
siRNA
Ctrl.
PIP5Kγ
F-Actin
HeLa
D
PIP5Kγ
+/+
-/-
F-Actin
MEFs

Figure 3. PIP5Kγ depletion or knockout generates a distinct actin phenotype. (A) HeLa cells were transfected with siRNA directed against PIP5Kα, PIP5Kβ, PIP5Kγ pan, PIP5Kγ90, or control (Ctrl.). 48 hours (PIP5Kβ) or 72 hours post-transfection, cells were analyzed via fluorescence images with FITC-phalloidin staining. Images were obtained by Dr. Ying-Jie Wang. Data shown is representative of multiple experiments performed over a period of 2 years. (B and C) HeLa cells were analyzed 72 hours post-transfection with either PIP5Kγ pan siRNA directed against a common region in PIP5Kγ90 and γ87 or control (Ctrl.) siRNA. (B) Immunoblot. (C) Fluorescence images with TRITC-phalloidin staining. (D) Fluorescence images. *PIP5Kγ* +/+ and *PIP5Kγ* -/- MEFs were stained with TRITC-phalloidin. Images were obtained by Xiaohui Zhu. Data shown is representative of MEFs isolated from at least three different mice for each group.

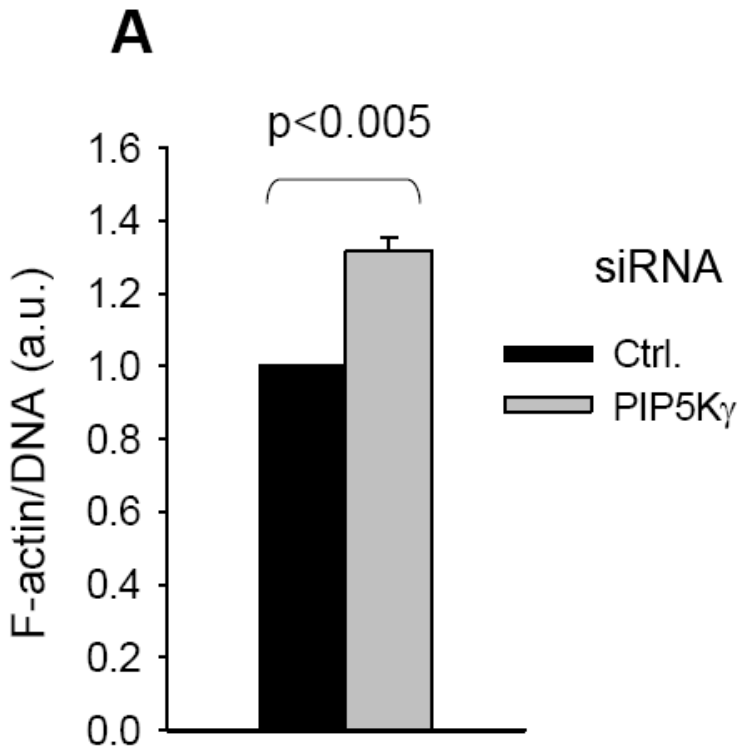
A
p<0.005
1.6
1.4
1.2
1.0
0.8
0.6
0.4
0.2
0.0
F-actin/DNA (a.u.)
siRNA
Ctrl.
PIP5Kγ

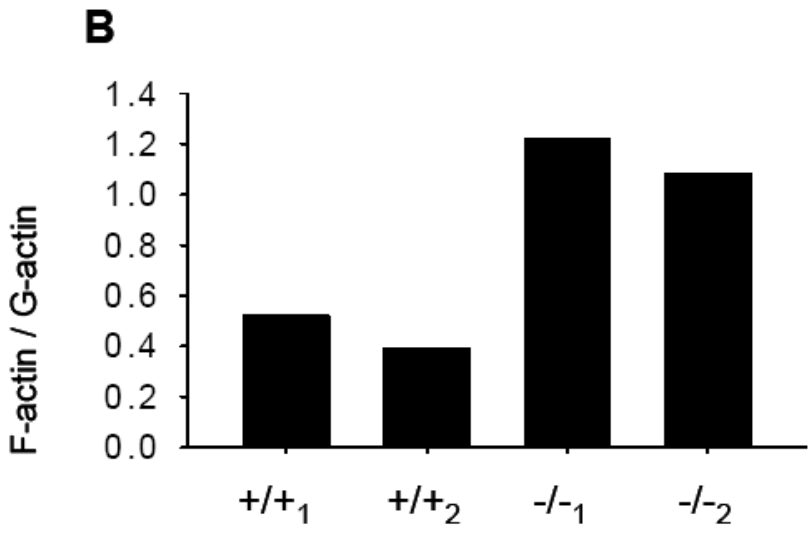
B
1.4
1.2
1.0
0.8
0.6
0.4
0.2
0.0
F-actin / G-actin
+/+1
+/+2
-/-1
-/-2

Figure 4. Cells with decreased or no PIP5Kγ have more polymerized actin. (A) HeLa cells were analyzed 72 hours post-transfection with either PIP5Kγ pan siRNA directed against a common region in PIP5Kγ90 and γ87 or control (Ctrl.) siRNA. Fluorometric F-actin quantitation (mean ± s.e.m., n=5). (B) Quantitation of TX-100 soluble and insoluble actin pools. Two different sets of *PIP5Kγ* +/+ and *PIP5Kγ* -/- MEFs were extracted with TX-100, and the amount of actin in the soluble and insoluble fractions was determined by Western blotting and densitometry. The ratios of actin in the insoluble fraction (F-actin) to actin in the soluble fraction (G-actin) are plotted on the Y-axis. Data was obtained by Xiaohui Zhu.

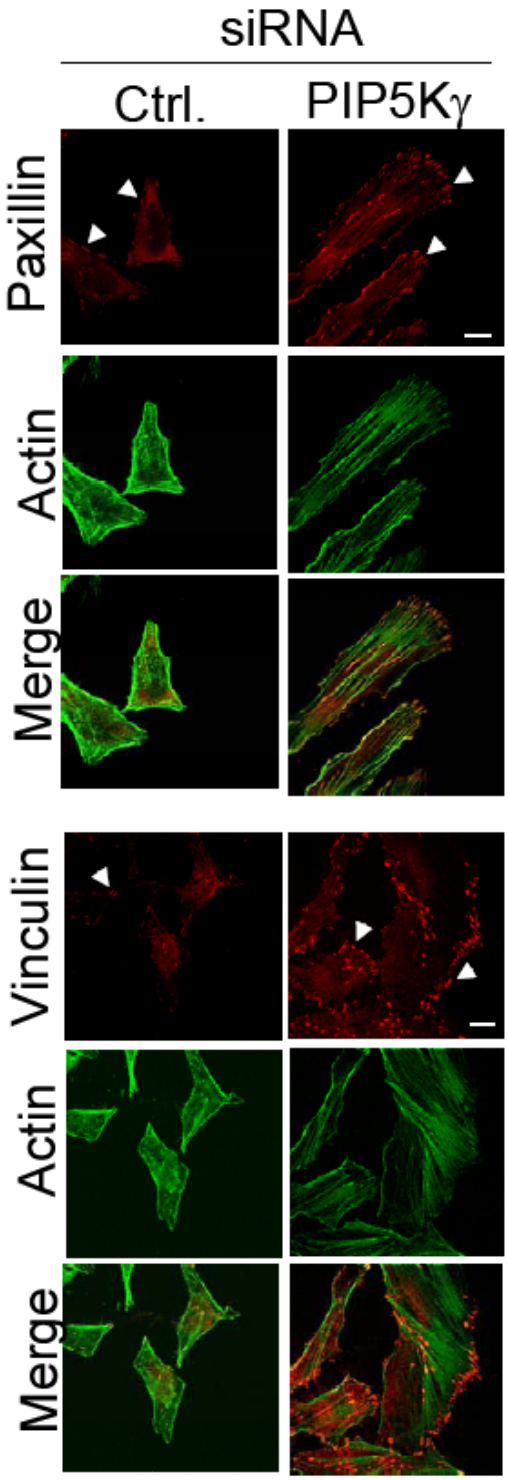
siRNA
Ctrl.
PIP5Kγ
Paxillin
Actin
Merge
Vinculin
Actin
Merge

Figure 5. PIP5Kγ depleted cells have more prominent FAs. HeLa cells were analyzed 72 hours post-transfection with either PIP5Kγ pan siRNA or control (Ctrl.) siRNA and labeled with phalloidin (green) and antibodies to either paxillin or vinculin (red). Arrowheads indicate selected FAs.

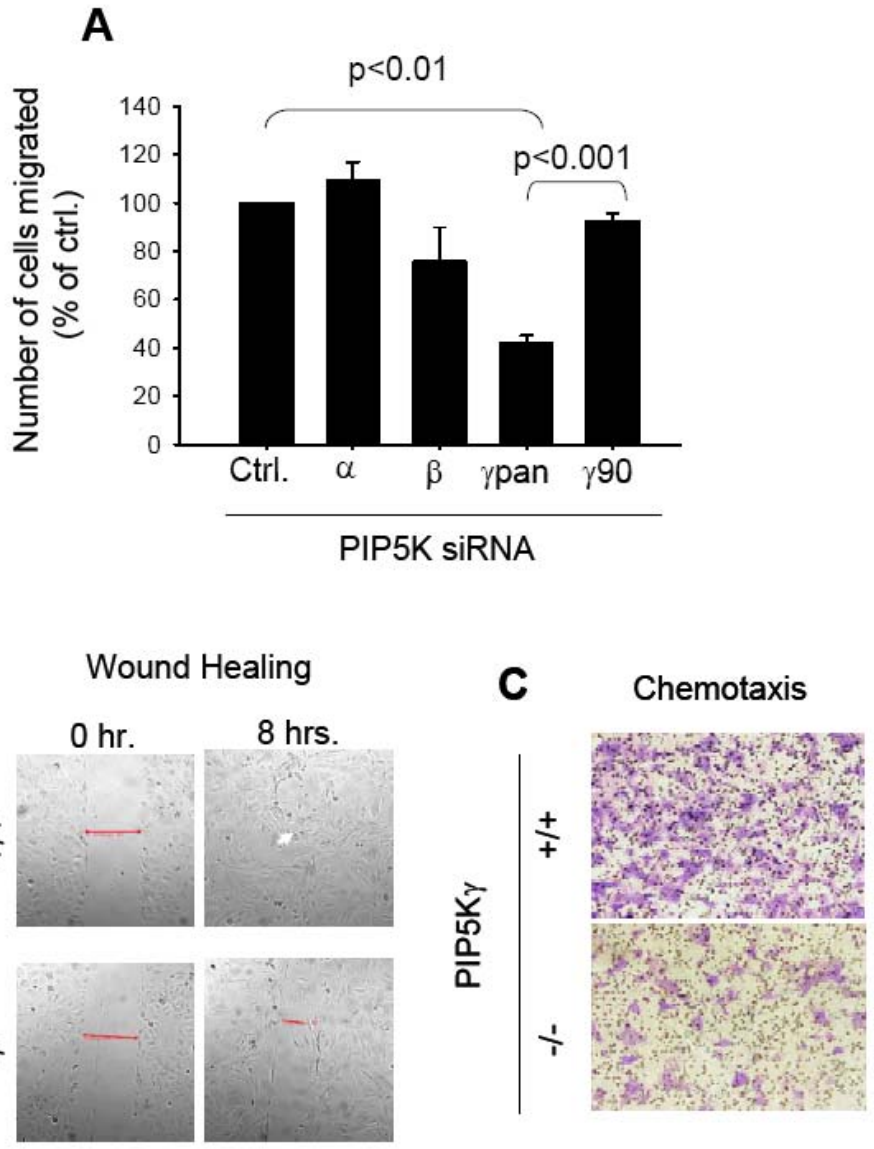
A
p<0.01
p<0.001
Number of cells migrated
(% of ctrl.)
140
120
100
80
60
40
20
0
Ctrl.
α
β
γpan
γ90
PIP5K siRNA
B
Wound Healing
0 hr.
8 hrs.
PIP5Kγ
+/+
-/-
C
Chemotaxis
PIP5Kγ
+/+
-/-

Figure 6. PIP5Kγ depletion inhibits chemotaxis and wound healing. (A) HeLa cell transwell chemotactic motility assay. After siRNA transfection, the number of HeLa cells which migrated from a serum-free compartment towards a serum-containing compartment was quantitated. Data was obtained by Dr. Ying-Jie Wang (mean ± s.e.m., n=3). (B) MEF wound healing assay. Confluent MEF monolayers were wounded with a scratch and the width of the "wound" (indicated by the red line) was determined immediately after wounding and 8 hours later. The black arrowhead indicates the site of initial wounding. Data was obtained by Xiaohui Zhu. (C) MEF transwell chemotactic motility assay. Images depict cells that have migrated from the serum-free top well through the filter towards the serum-containing bottom well. Cells on the lower face of the filter are stained with crystal violet and appear purple (the black circles are the pores on the filter). Magnification is 200×. Data was obtained by Xiaohui Zhu.

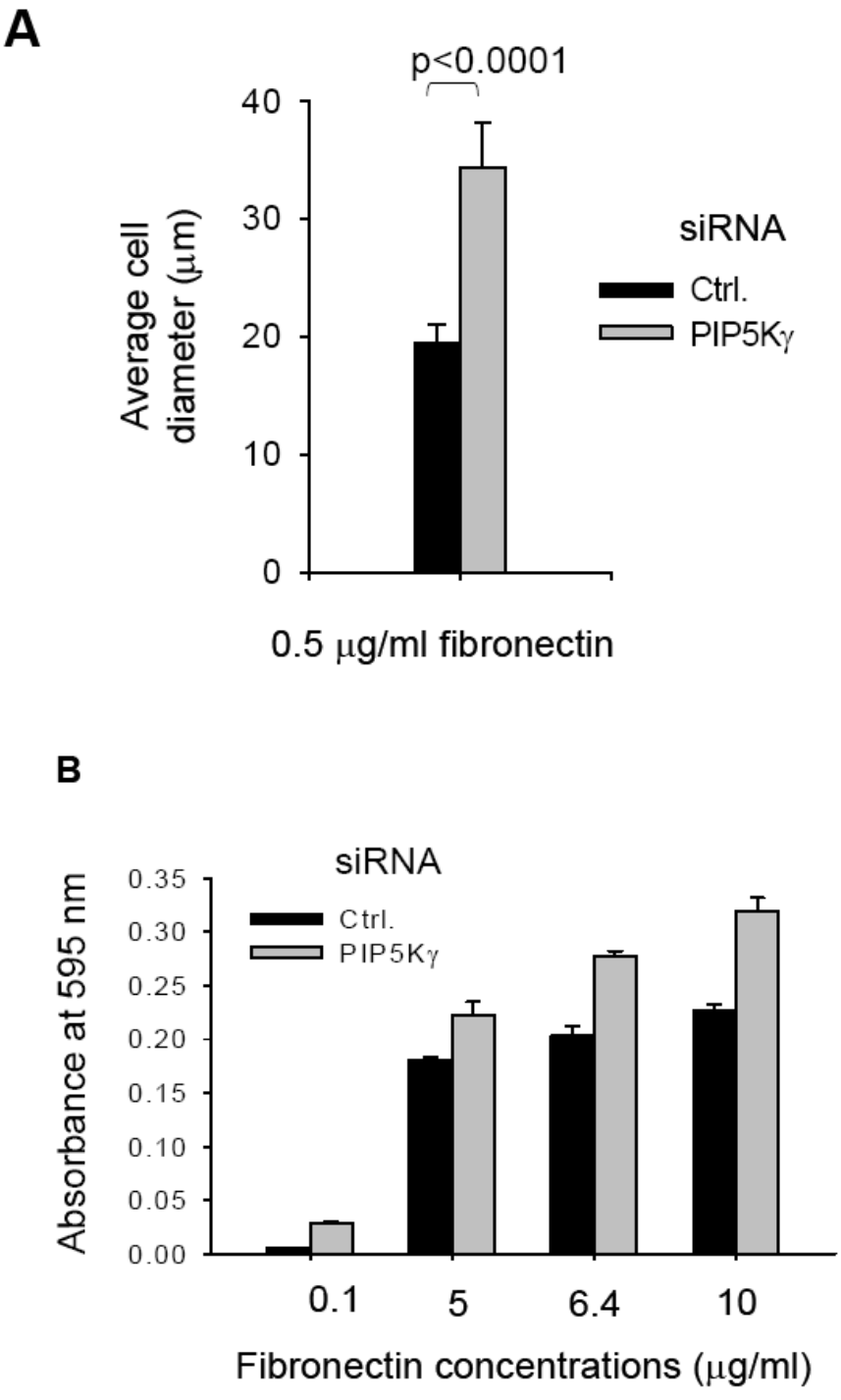
A
p<0.0001
40
30
20
10
0
Average cell diameter (μm)
siRNA
Ctrl.
PIP5Kγ
0.5 μg/ml fibronectin
B
siRNA
Ctrl.
PIP5Kγ
0.35
0.30
0.25
0.20
0.15
0.10
0.05
0.00
Absorbance at 595 nm
0.1
5
6.4
10
Fibronectin concentrations (μg/ml)

Figure 7. PIP5Kγ depletion results in enhanced adhesion to fibronectin substrate. (A) Cell spreading. Cells were allowed to spread on 0.5 μg/ml fibronectin-coated surface for 1 hour and their diameters were measured at the widest part of the cell (mean ± s.e.m., n=21 cells each). (B) Cell attachment. Cells were seeded on surfaces coated with increasing amounts of fibronectin for 1 hour and were stained with crystal violet dye. The intensity of cell-associated dye was quantitated. Data shown are representative of 3 independent experiments.

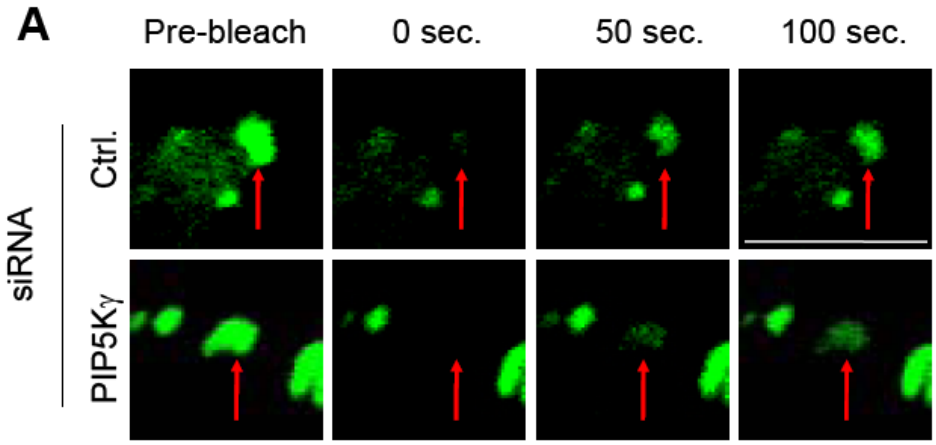
A
Pre-bleach
0 sec.
50 sec.
100 sec.
siRNA
Ctrl.
PIP5Kγ

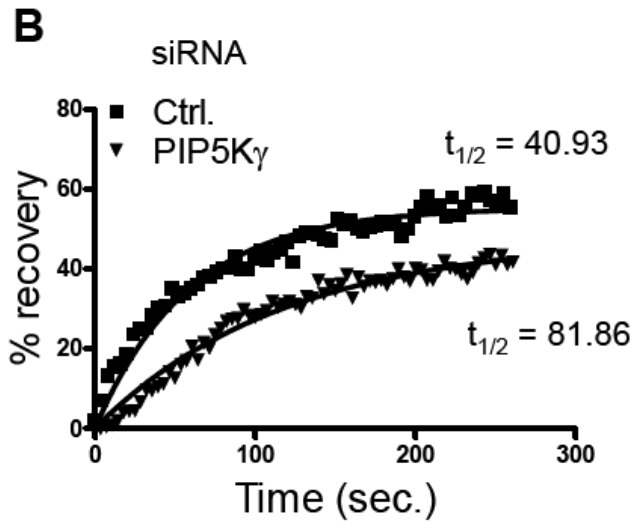
B
siRNA
Ctrl.
PIP5Kγ
t1/2 = 40.93
t1/2 = 81.86
% recovery
80
60
40
20
0
0
100
200
300
Time (sec.)

Figure 8. PIP5Kγ depleted cells have more static FAs. FRAP of GFP-paxillin or -vinculin. (A) Representative images of GFP-paxillin expressing cells before and at varying time points after bleaching. Red arrows indicate the region that was bleached. (B) Analysis of this experiment was depicted in an exponential curve fit containing both % recovery and $t_{1/2}$ data.

FRAP Averages

siRNA	Vinculin			Paxillin		
	$t_{1/2}$	% recovery	n	$t_{1/2}$	% recovery	n
Ctrl.	39 sec. ± 6	55 ± 4	8	39 sec. ± 3	55 ± 4	13
PIP5Kγ	83 sec. ± 9	53 ± 4	12	71 sec. ± 8	37 ± 3	19

Table 1. Summary of GFP-paxillin and GFP-vinculin FRAP data.

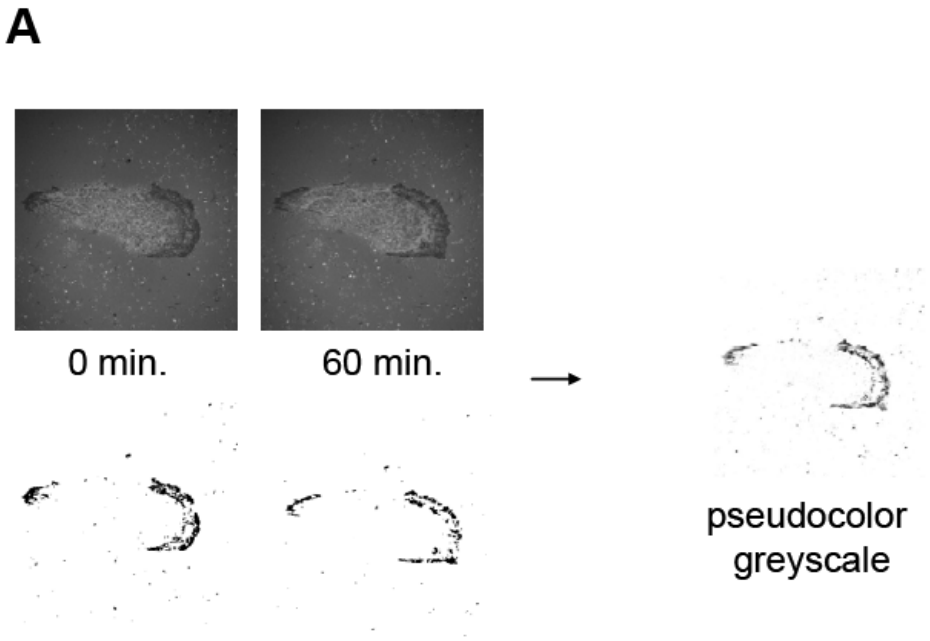
A
0 min.
60 min.
pseudocolor
greyscale
B
0 min.
60 min.
siRNA
Ctrl.
PIP5Kγ
4.589 ± 0.412
2.197 ± 0.249

Figure 9. PIP5Kγ depleted cells have a lower FA turnover index as determined by IRM. (A) Method for calculating FA turnover index. Cells were imaged by time lapse for 60 minutes. IRM images from the first and last time points are displayed (upper right panels). Individual images were filtered and thresholded to display only the dark FAs (bottom right panels). Left, images from each time point were overlayed, and the changes in FA location between frames were scored and displayed as a pseudocolor greyscale. (B) Turnover index was calculated from the ratio of light grey pixels to dark grey pixels (areas of high and low FA variability between time points, respectively). Images from 0 and 60 min. are shown, and the calculated FA turnover indexes are shown at the right hand corner of the 60 min. panel (n=15).

CHAPTER 3: MECHANISTIC INSIGHT INTO THE ROLE OF PIP5K GAMMA ON THE STRONG STRESS FIBER AND FOCAL ADHESION PHENOTYPE

I. Differentiating the Contributions of PIP5Kγ87 and PIP5Kγ90

In the majority of the experiments in Chapter 2, depletion of PIP5Kγ has been accomplished by siRNA directed against a site common to both the PIP5Kγ87 and PIP5Kγ90 splice variants (Fig. 10A). Although quantitative PCR has shown that PIP5Kγ87 is much more abundant than PIP5Kγ90 at the mRNA level (Wang et al., 2004), it is important to evaluate the contributions of the individual variants. We therefore used siRNA directed against the unique COOH-terminus of PIP5Kγ90 to exclusively deplete it (Fig. 10A). Loss of only PIP5Kγ90 resulted in an actin phenotype distinct from the PIP5Kγpan phenotype (Fig. 10B). PIP5Kγ90 depleted cells do not have the thick actin stress fibers found in PIP5Kγpan depleted cells and they look similar to cells treated with control siRNA. Furthermore, depletion of PIP5Kγ90 alone failed to produce the chemotactic migration defect that is found when both PIP5Kγ splice varients were depleted (Fig. 6A, compare γpan and γ90). These results indicate that the actin and migration phenotypes may be primarily due to the loss of PIP5Kγ87.

Continuing our pursuit to distinguish the effects of PIP5Kγ87 and 90, I next analyzed the ability of each splice variant to rescue the actin phenotype. PIP5Kγpan depleted HeLa cells were microinjected (Fig. 11A) or transfected (Fig. 11B) with GFP-labeled PIP5Kγ87, PIP5Kγ90, or a PIP5Kγ87 kinase dead (KD) mutant (Fig. 11C). GFP- PIP5Kγ87 rescued 86% of cells as compared to

the 19% rescued by GFP- PIP5Kγ87KD or the 16% rescued by GFP alone. This indicates that while GFP- PIP5Kγ87 is sufficient to rescue the actin phenotype of the PIP5Kγpan depleted cells, the GFP-PIP5Kγ87KD mutant is not, signifying that the actin rescue is PIP_2 dependent. Paradoxically, although PIP5Kγ90 depletion does not generate robust actin stress fibers, the GFP-PIP5Kγ90 was also able to rescue the actin phenotype.

Simmilar results were obtained by transducing either WT or KD GFP- PIP5Kγ87 retrovirus into *PIP5Kγ -/-* MEFs (Fig. 11C). PIP5Kγ87 transduction decreased the robust actin stress fibers in 40% of the *PIP5Kγ -/-* MEFs, while PIP5Kγ87KD did not. Thus, PIP5Kγ87 is able to partially rescue and kinase activity appears to be required for restoring normal actin organization (Fig. 11D). At this time, we are not sure why the extent of rescue by PIP5Kγ87 in the *PIP5Kγ -/-* MEF cells is less than that of the PIP5Kγ depleted HeLa cells, but it may be related to lower levels of overexpression.

II. The PIP5Kγ RNAi Actin Phenotype in HeLa Cells is Mediated Through the Rho/ROCK/Myosin Pathway

We strove to elucidate the mechanism by which PIP5Kγ depletion generates the characteristic actin phenotype in HeLa cells. Excessive RhoA activation is known to result in an increase in actin stress fibers and FAs, similar to the phenotype of PIP5Kγ depleted cells (Ridley et al., 1992). RhoA activates its downstream effector ROCK, which in turn facilitates phosphorylation of myosin light chain, both by direct phosphorylation and inhibition of a myosin phosphatase (Leung et al., 1995, Ishizaki et al., 1996, Amano et al., 1996, Matsui 1996, Kimura et al., 1996, Uehata et al., 1997) (Fig. 14).

First, I considered the contributions of myosin II by employing blebbistatin (Straight et al., 2003), a myosin II inhibitor that stabilizes myosin II in a conformation with low affinity for actin (Kovacs et al., 2004). Upon myosin inhibition, the RNAi actin phenotype was rescued (Fig. 12A). Having discovered that the stress fiber phenotype appears to be myosin dependent, I continued our line of inquiry by inhibiting ROCK, an upstream regulator of myosin. Accordingly, I found that inhibition of ROCK by Y-27632 was also able to rescue the actin phenotype, implicating ROCK in mediating the actin phenotype (Fig. 12B). To advance our understanding of mechanisms regulating the actin phenotype, I investigated the function of Rho in this pathway. Treatment of PIP5Kγ depleted cells with C3 transferase, a RhoA inhibitor, rescued the actin phenotype (Fig. 12C).

Since our results implicated the involvement of Rho and previous studies have shown that *PIP5Kγ -/-* bone marrow macrophages have increased levels of Rho (Mao et al., 2009), I next examined Rho activation. Using a RhoA G-LISA assay, I found that PIP5Kγ depleted HeLa cells contain more activated RhoA (Fig. 13). We conclude that PIP5Kγ depletion induces robust actin stress fibers through Rho, ROCK, and myosin dependent mechanisms.

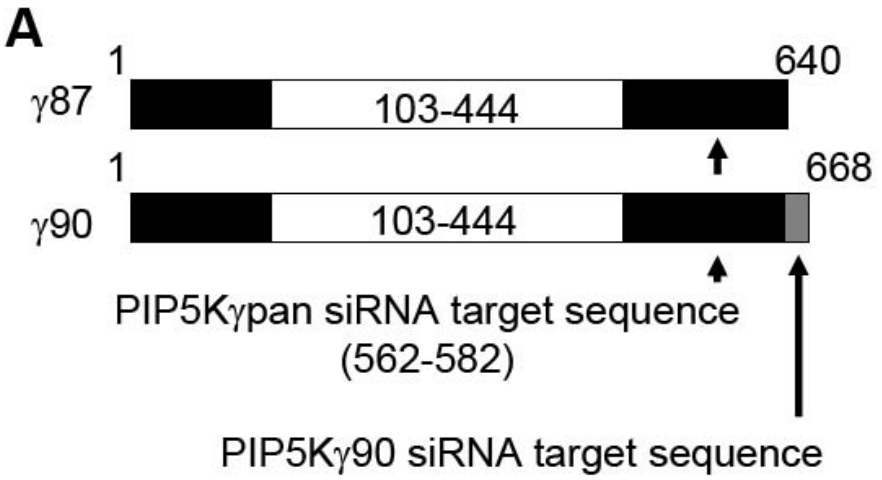
A
1
640
γ87
103-444
1
668
γ90
103-444
PIP5Kγpan siRNA target sequence
(562-582)
PIP5Kγ90 siRNA target sequence

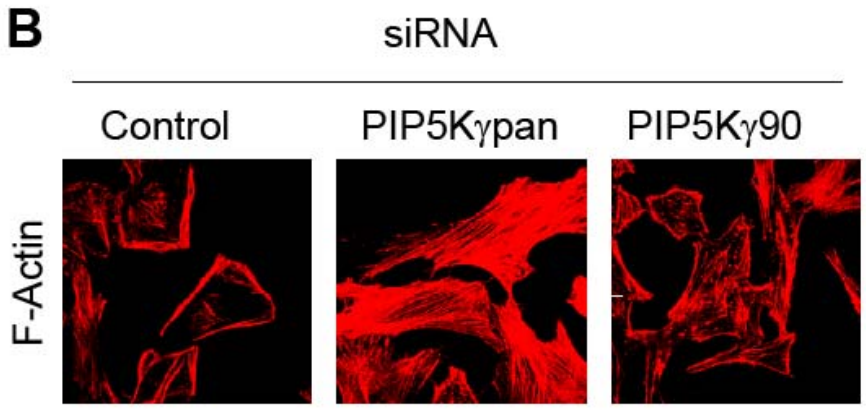
B
siRNA
Control
PIP5Kγpan
PIP5Kγ90
F-Actin

Figure 10. Differentiating the effects of PIP5KIγ90 and PIP5KIγ87 on the actin phenotype. (A) Scheme of siRNA targeting sites in PIP5Kγ87 and γ90. PIP5Kγ pan siRNA is directed against a common region in both variants, while γ90 siRNA is only targeted to the unique COOH-terminus of γ90. (B) Fluorescence images. HeLa cells, after transfection with siRNA, were stained with TRITC-phalloidin.

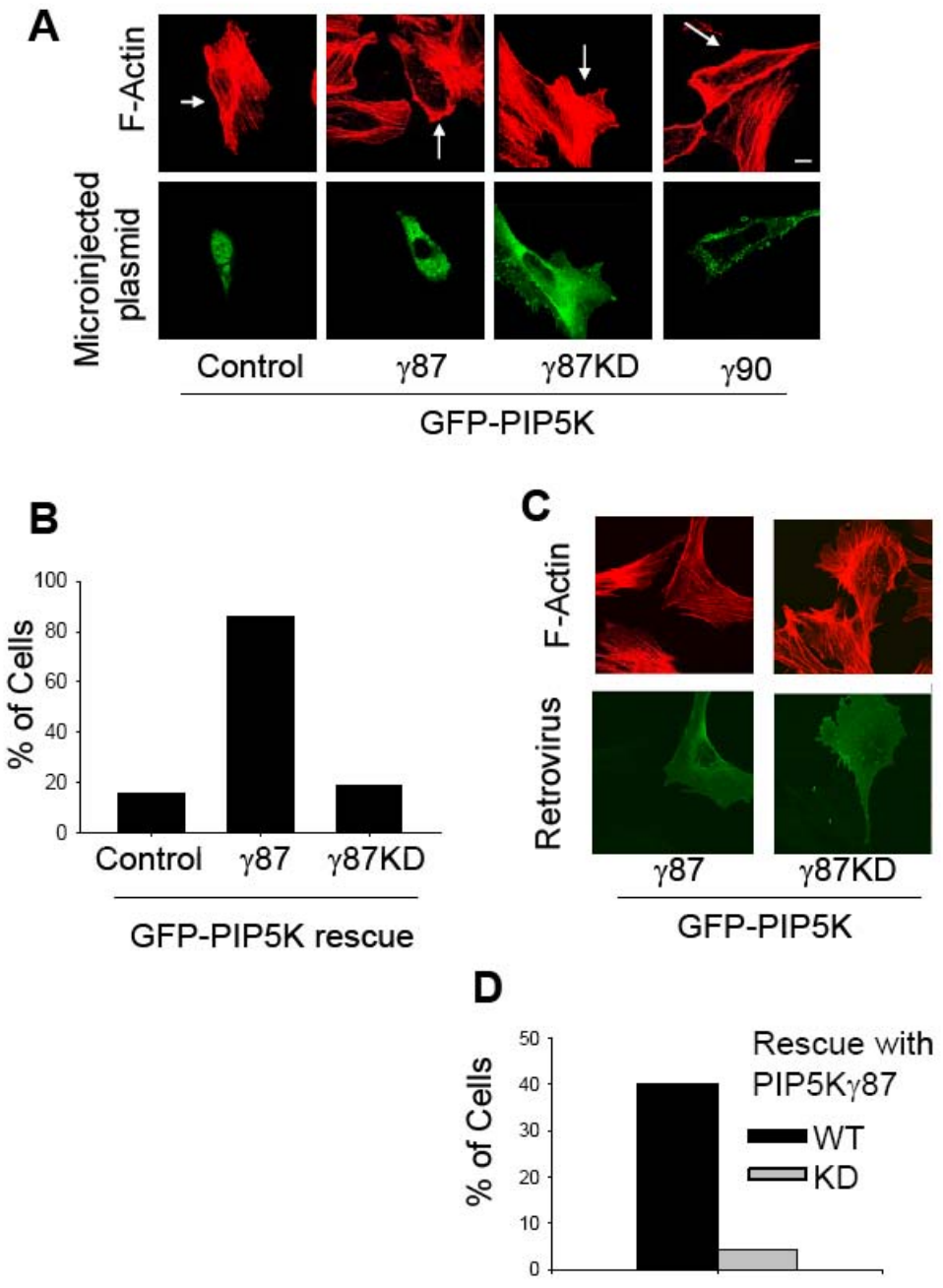
A
F-Actin
Microinjected plasmid
Control
γ87
γ87KD
γ90
GFP-PIP5K
B
% of Cells
100
80
60
40
20
0
Control
γ87
γ87KD
GFP-PIP5K rescue
C
F-Actin
Retrovirus
γ87
γ87KD
GFP-PIP5K
D
% of Cells
50
40
30
20
10
0
Rescue with PIP5Kγ87
WT
KD

Figure 11. PIP5Kγ87 is sufficient to rescue the actin phenotype casued by depletion of both PIP5Kγ isoforms. (A and B) Rescue of the PIP5Kγpan RNAi actin phenotype. Cells that had been transfected with PIP5Kγ pan siRNA were microinjected (A) or transfected (B) with GFP, GFP-PIP5Kγ87, GFP-γ87D136K (kinase dead), or GFP-γ90, fixed, and stained with TRITC-phalloidin (A) n=16 cells for control, n=28 for γ87, n=7 for γ87KD, and n=65 for γ90 (B) n=99 cells for control, n=55 for γ87, and n=32 for γ87KD. (C) Rescue of the *PIP5Kγ -/-* MEF actin phenotype. *PIP5Kγ -/-* MEF cells were transduced with either GFP-PIP5Kγ87 or γ87KD retrovirus, fixed, and stained with TRITC-phalloidin. (D) Quantitation of rescue data. The actin phenotype of transduced cells was considered rescued if they had appreciably weaker actin staining than surrounding cells (n=88 cells for γ87 and n=48 for γ87KD).

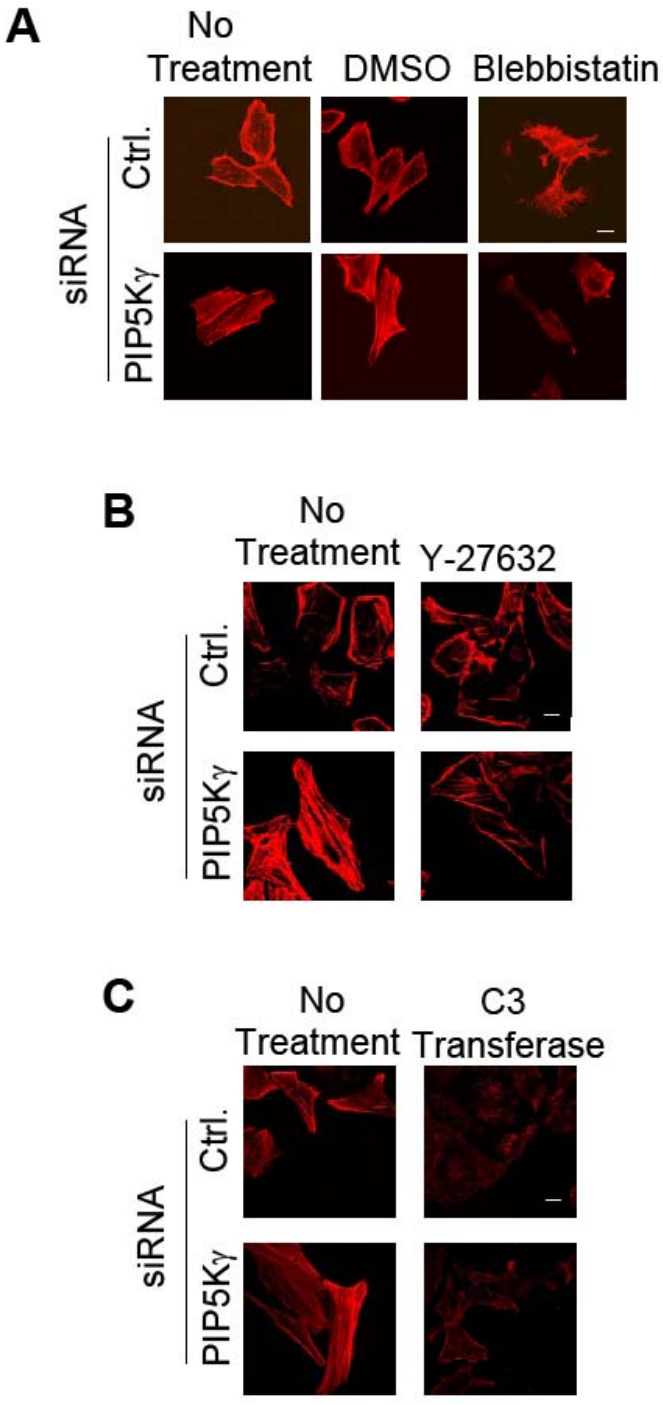
A
No Treatment
DMSO
Blebbistatin
siRNA
Ctrl.
PIP5Kγ
B
No Treatment
Y-27632
siRNA
Ctrl.
PIP5Kγ
C
No Treatment
C3 Transferase
siRNA
Ctrl.
PIP5Kγ

Figure 12. Rho/ROCK/Myosin pathway is involved in the PIP5Kγ RNAi actin phenotype in HeLa cells. (A) Blebbistatin, a myosin inhibitor, rescued the actin phenotype. Cells transfected with siRNA were incubated with 40 μM Blebbistatin or 1.17% DMSO for 1 hr., fixed, and stained with TRITC-phalloidin. (B) Y-27632, a ROCK inhibitor, rescued the actin phenotype. PIP5Kγpan depleted or Ctrl. cells were incubated with Y-27632 for 45 min., fixed, and stained with TRITC-phalloidin. (C) C3 transferase, a RhoA inhibitor, rescued the actin phenotype. PIP5Kγpan depleted or Ctrl. cells were incubated with 2.4 μg/ml cell permeable C3 transferase for 2 hrs., fixed, and stained with TRITC-phalloidin.

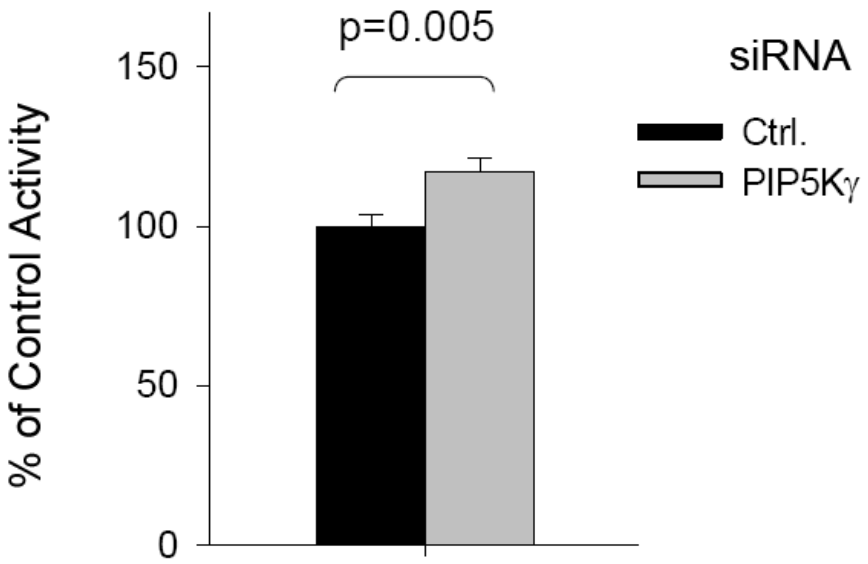
p=0.005
siRNA
Ctrl.
PIP5Kγ
% of Control Activity
150
100
50
0

Figure 13. Loss of PIP5Kγ increases the RhoA activation level, as determined by quantitation of GTP-Rho. PIP5Kγpan depleted or Ctrl. HeLa cell lysates were subjected to a RhoA G-LISA assay. Each individual experiment was done in triplicate and activity levels were calculated as % of Ctrl. cells (mean ± s.e.m., n=3).

CHAPTER 4: MATERIALS AND METHODST

Tissue Culture

Cells were cultured in DMEM with 10% fetal bovine serum, 10mM HEPES, 1mM sodium pyruvate, 100 units/ml penicillin, and 100 μg/ml streptomycin at 37°C in 5% CO_2.

Transfection

Cells were transiently transfected using Lipofectamine 2000 at a DNA concentration of 0.4 μg/well of a 12-well plate.

Immunoflourescence

Cells were grown on glass coverslips, fixed with 3.7% formaldehyde, permeabilized with 0.1% Triton X-100 on ice, and labeled with antibodies in blocking buffer (1% BSA, 3% donkey serum in PBS). Images were collected with a Zeiss Laser Scanning Confocal Microscope 510 using a 63X/ 1/3NA PlanApo objective.

Cell Adhesion Assay

Experiments were preformed similar to Kueng et al. (1998). Wells of a 96 well plate were incubated with the indicated concentration of fibronectin for 1 hr. at room temperature. Wells were then incubated with 10 mg/ml heat-denatured BSA for 1 hr. at room temperature. HeLa cells in serum free media were added to each well and incubated for 1 hr. at 37°C in 5% CO_2. Wells were gently tapped, fixed with 3.7% paraformaldehyde, washed 3 times with water, and incubated with 100 μl/well of 0.1% (w/v) crystal violet solution for 1 hr. at room

temperature. Wells were washed 3 times with water and incubated with 100 µl/well of 10% (v/v) acetic acid for 5 min. while shaking at room temperature. Absorbance was measured at 595 nm.

Cell Spreading Assay

Experiments were preformed similar to Yamada et al. (1984). Glass coverslips were coated with the indicated concentration of fibronectin for 1 hr. at room temperature. Wells were then incubated with 10 mg/ml heat-denatured BSA for 1 hr. at room temperature. HeLa cells in serum free media were added to each well and incubated for 1 hr. at 37°C in 5% CO_2. Cells were fixed and stained with TRITC-phalloidin and examined by confocal microscopy. Cell diameters were measured at the widest part of the cell.

Immunofluorescence F-actin Measurement

Experiments were preformed similar to Cox et al. (1996). HeLa cells in a 24-well plate were fixed with 3.7% formaldehyde, permeabilized with 0.1% Triton X-100, and labeled with FITC-phalloidin and DAPI in blocking buffer (3% donkey serum and 1% BSA in PBS). Plates were excited at 360 nm and 480 nm wavelengths and read at 460 nm and 530 nm respectively. Background autofluorescence was subtracted and the ratio of FITC/DAPI fluorescence intensity was calculated.

Microinjections

GFP-PIP5K DNA plasmid was diluted to 0.1 µg/ µl with Milli-Q water and centrifuged for 20 min. to remove particulates and was added to a microinjection needle. Cells grown on glass coverslips were placed in a 35mm dish and plasmid was injected into cell nuclei during a 10 min. period. Cells were incubated for 2-4 hrs. at 37°C in 5% CO_2.

PIP5K Depletion by Small Interfering RNA (siRNA)

Cells in a 6-well dish were transfected with 10 nmol siRNA using Oligofectamine. We use the human PIP5K isoform designation (Mao et al., 2007). PIP5Kα and γ siRNA transfected cells were used 72 hrs. later and PIP5Kβ siRNA transfected cells were used 48 hrs. later. The siRNA sequences used were the same as in Padron et al. (2003): PIP5Kα (nucleotides 1923-1943), PIP5Kβ (nucleotides 1114-1135), and PIP5Kγ (nucleotides 619-639). An siRNA sequence targeting firefly luciferase (nucleotides 695-715) was used as a control.

Triton Soluble/Insoluble F-actin Fractionation

Fractionation was carried out at 4ºC. Cells in a 6-well plate were washed with wash buffer (20 mM PIPES, 40 mM KCL, 5 mM EGTA, 1 mM EDTA). Cells were lysed in 200 µl of lysis buffer/well (20 mM PIPES, 40 mM KCL, 5 mM EGTA, 1 mM EDTA, 1% Triton X 100, protease inhibitor). Cells were lifted and centrifuged at 14,000 RPM for 25 min. and the pellet was resuspended in 40 µl of resuspension buffer (20 mM PIPES, 40 mM KCL, 5 mM EGTA, 1 mM EDTA, 1% Triton X 100, protease inhibitor, 100 mM sucrose, 0.2 mM DTT).

RhoA Activity

GTP-RhoA was detected using the colorimetric RhoA G-LISA specific Activator Assay manufactured by Cytoskeleton, Inc. (Cat #BK124). Either 1.0 or 1.3 µg/ml total protein concentration was used for the assay.

Interference Reflection Microscopy

Experiments were preformed similar to Saunder et al. (2006). Live HeLa cells were imaged by time lapse for 1 hr. at 37ºC using an Applied Precision

Deltavision RT deconvolution microscope. Images were processed using Image J software.

Flourescence Recovery After Photobleaching

Experiments were performed similar to Chandrasekar, et al. (2005). HeLa cells which had been transfected or microinjected were placed on a 37ºC stage and allowed to equilibrate for 20 min. before viewing. Indicated regions were photobleached using 50 iterations of the 488 nm laser at 100%. Time lapse images were collected and the fluorescence intensity of the bleached region at each time point was calculated using the Metamorph Image software.

Retrovirus Transduction

MEF cells in a 6-well plate were incubated with 0.5 ml virus and 1.5 ml media per well for 5 hrs. at 37°C in 5% CO_2. Two additional ml of media were added and the plate was incubated over night at 37°C in 5% CO_2. Cells were replated onto coverslips, cultured for another 24 hours, and then fixed and stained with TRITC-phalloidin.

MEF Cell Preparation

Mef cells were generated by isolating day 15.5 – 16.5 postcoitum mouse embryos, mincing them, and creating a cell suspension by incubating with 0.25% trypsin/EDTA and subjecting them to shear force with a 3 cc syringe.

Wound Healing Assay

MEF cells were plated in a 35mm MatTek dish at a density of 5 x 10^5 cells/dish. Cells were wounded with a scratch and images were captured at indicated times.

Cell Migration Assay

Experiments were performed similar to the methods described by Wei et al. (2002) and Arthur et al. (2001). 0.5 ml of DMEM with 10% fetal bovine serum was placed in the lower compartment of a 6.5-mm polycarbonate transwell filter with 8-μm pores (Corning Costar, Cat. No. 3442). HeLa cells were resuspended at a concentration of 2.0 x 10^5 cells/ml in DMEM with 1% BSA and 100 μl of the cell suspension were added to the upper surface of the filter. Cells were allowed to migrate for 4 hrs. at 37°C in 5% CO_2. Membrane filters were fixed in 3.7% formaldehyde and cells were stained with coomassie brilliant blue G. Total number of cells migrated are the average of 5 fields. MEF cells were assayed similarly, but with the following changes: the filter was precoated with 5 μg/mL fibronectin overnight and cells were fixed with methanol and stained with crystal violet for 20 min. at room temperature.

Antibodies, DNA Constructs, and Reagents

Antibody to PIP5Kγ was a gift from Dr. Pietro De Camilli (Yale University). GFP-vinculin plasmid was a gift from Dr. Susan Craig (Johns Hopkins University) and GFP-paxillin plasmid was a gift from Dr. Chris Turner (SUNY). Cell permeable C3 transferase was purchased from Cytoskeleton. HRP-conjugated secondary antibodies were purchased from GE Healthcare and fluorescent-conjugated secondary antibodies were purchased from Jackson ImmunoResearch Laboratories. Antibody to actin was purchased from Millipore, antibody to vinculin was purchased from Sigma (Cat #V4505), and antibody to paxillin was purchased from Upstate (Cat #05-417).

CHAPTER 5: DISCUSSION AND FUTRE DIRECTIONS

Our data suggests that PIP5Kγ87 regulates actin stress fiber formation and FA dynamics. We find that PIP5Kγ depleted HeLa cells have more F-actin and more prominent FAs with slower turnover rates than control cells, are more adherent and spread more on fibronectin coated surfaces, and display slower chemotactic migration. These results were recapitulated in *PIP5Kγ -/-* MEFs, which also have increased F-actin and decreased motility compared to *PIP5Kγ +/+* MEFs.

PIP_2 plays an essential role in FA dynamics. Sequestering of PIP_2 by microinjection of a monoclonal antibody has been shown to inhibit stress fiber and FA formation (Gilmore et al., 1996) and overexpression of pleckstrin homology domains to sequester PIP_2 leads to a decrease in cell adhesion (Martel et al., 2001). Binding of PIP_2 to talin enhances the interaction between talin and β integrin, an important step in FA formation (Martel et al., 2001, Goksoy et al., 2008). Expression of mutant vinculin which is unable to bind to PIP_2 results in highly stable FAs, indicating the importance of PIP_2 in FA disassembly (Chandrasekar et al., 2005, Saunders et al. 2006). The FA phenotype of PIP5Kγ depleted cells indicates that the pool of PIP_2 produced by PIP5Kγ87 is particularly important for FA disassembly.

We find that depletion of PIP5Kγ90 alone is not sufficient to cause this phenotype, suggesting that the PIP5Kγpan siRNA phenotype is primarily due to loss of PIP5Kγ87. However, paradoxically, forced PIP5Kγ90 overexpression is able to rescue the actin phenotype of PIP5Kγpan siRNA cells. One potential explanation for this discrepancy is that PIP5Kγ87 is the only isoform critical to

FA disassembly. If this is the case, it is probable that as PIP5Kγ90 is present at such low levels in HeLa cells initially (Wang et al., 2004), the introduction of GFP-PIP5Kγ90 causes expression levels so high in excess of basal levels that it results in mislocalization of PIP5Kγ90 to discrete areas where normally only PIP5Kγ87 would be recruited.

An alternative possibility is that PIP5Kγ90 and PIP5Kγ87 play redundant roles in the disassembly of FAs, as suggested by the rescue assays. If this is the indeed the mechanism, the inability of PIP5Kγ90 specific depletion to cause the distinctive actin phenotype may again be explained by the low basal levels of PIP5Kγ90 in HeLa cells (Wang et al., 2004). As it is present in such higher amounts, PIP5Kγ87 may be able to compensate for the loss of PIP5Kγ90.

Although PIP5Kγ90 is enriched in FA and is known to be important to FA assembly through its interactions with talin (Di Paolo et al., Ling et al., 2002), far less is known about the role of PIP5Kγ87 in FAs. Powner et al. (2005) have suggested that PIP5Kγ87 generated PIP_2 is necessary for initial cell adhesion and PIP5Kγ90 is then involved in the ensuing FA formation and maturation. Our results are significant in that they are some of the first evidence that PIP5Kγ87 is involved in the regulation of FA disassembly. Notably, a kinase dead PIP5Kγ87 mutant was unable to rescue the actin phenotype of PIP5Kγpan depleted HeLa cells, indicating that the increase in actin stress fibers is due to the loss of PIP_2 generated by PIP5Kγ87.

Previously, it has been reported that in rat basophilic leukemic-2H3 cells, overexpression of either PIP5Kγ87 or PIP5Kγ93 led to an increase in adhesion to a serum coated plate, an effect that was not seen upon overexpression of

PIP5Kγ90 or PIP5Kγ87KD (Powner et al., 2005). Although this is seemingly at odds with our conclusion that PIP5Kγ87 is important for the disassembly of FAs, the difference may be attributed to either to cell line specific variations or an indirect result of the method used by Powner et al. (2005). High overexpression levels of PIP5Kγ87 may have resulted in a non-physiological localization pattern.

Although RhoA and Rac1 have long been known to regulate the activity of the PIP5Ks (Chong et al., 1994, Tolias et al., 1995, Oude Weernink et al., 2000, Oude Weernink et al., 2004), Mao et al. (2009) provided compelling evidence that PIP5Kγ also acts upstream of Rac and RhoA. They find that *PIP5Kγ-/-* bone marrow macrophages contain increased amounts of GTP-RhoA and decreased amounts of GTP-Rac (Mao et al., 2009). Furthermore, manipulation of the Rac and RhoA activation levels, either through chemical inhibition or vector expression, is able to rescue a particle attachment defect during phagocytosis that is caused by the absence of PIP5Kγ (Mao et al., 2009). Our finding that RhoA activity levels are elevated in PIP5Kγ depleted cells and C3 transferase, a RhoA inhibitor, rescues the actin phenotype, are in agreement with the model of Mao et al. (2009). Although we attempted to examine if there were any salient differences in Rac activation, the levels of active Rac in our HeLa cells were too low to detect any discernable changes using a Rac G-LISA assay. We hypothesize that PIP5Kγ regulates the actin cytoskeleton by inhibiting RhoA (Fig. 14).

ROCK is a downstream effector of RhoA (Leung et al., 1995, Ishizaki et al., 1996, Matsui 1996), and it regulates many important cellular functions. Here we investigated its role in the robust stress fiber phenotype in PIP5Kγ depleted cells. ROCK increases myosin light chain phosphorylation in at least two ways: first, by

direct phosphorylation of myosin light chain (Amano et al., 1996), and second, by inactivating myosin phosphatase (Kimura et al., 1996, Uehata et al., 1997). Myosin II induces contraction of stress fibers, and the mechanical forces regulate FA formation, maturation, and disassembly (Rottner et al., 1999, Webb et al., 2004, Gupton et al., 2006). We found that inhibition of ROCK with Y-27632 or inhibition of myosin with blebbistatin was able to rescue the PIP5Kγ depletion actin phenotype. Thus, we conclude that the PIP5Kγ depleted actin phenotype is due to abnormal RhoA activation and occurs in a ROCK and myosin dependent manner (Fig. 14).

Future studies will be directed toward further elucidating the mechanisms by which PIP5Kγ87 regulates FA turnover. Although it has long been theorized that internalization of β1 integrin is an important step in FA disassembly, it is only very recently that this assumption has been experimentally confirmed. Chao et al. (2009) compared the relative rates of FA disassembly and activated β1 integrin internalization in human fibrosarcoma cells and found that the time scales were similar. In addition, they found that inhibition of β1 integrin uptake was sufficient to block FA disassembly, providing direct evidence that β1 internalization is a critical step in FA disassembly (Chao et al., 2009). Powelka et al. (2004) find that overexpression of a dominant negative Arf6 in HeLa cells inhibits β1 integrin recycling. Furthermore, Li et al. (2005) identified Arf-GAP with coiled-coil, ANK repeat and PH domain protein 1 (ACAP1), a GAP for Arf6, as a critical regulator of β1 integrin recycling. In addition, Dunphy et al. (2006) presented evidence that BRAG2, an Arf6 GEF, inhibits the endocytosis of β1 integrin. Caswell et al. (2008) hypothesize that the regulation of β1 integrin trafficking by Arf6 is mediated through Arf6 regulation of the PIP5Ks and the resultant changes in PIP_2 levels. They suggest that BRAG2 activation of Arf6

results in an increase in local membrane PIP_2 levels and that this leads to internalization (Caswell et al., 2008). Thus, it is enticing to speculate that the activity of the PIP5Kγ87 isoform may play a role in β1 integrin trafficking. This theory becomes even more attractive when we take into account that integrin signaling is known to regulate RhoA activity (Ren et al., 1999, Cox et al., 2001). Future experiments will explore whether there are any differences in the time scale of β1 integrin internalization between WT cells and cells lacking PIP5Kγ. If no differences are found, it might be of interest to determine if there is any change in the recycling of endocytosed β1 integrin back to the cell surface.

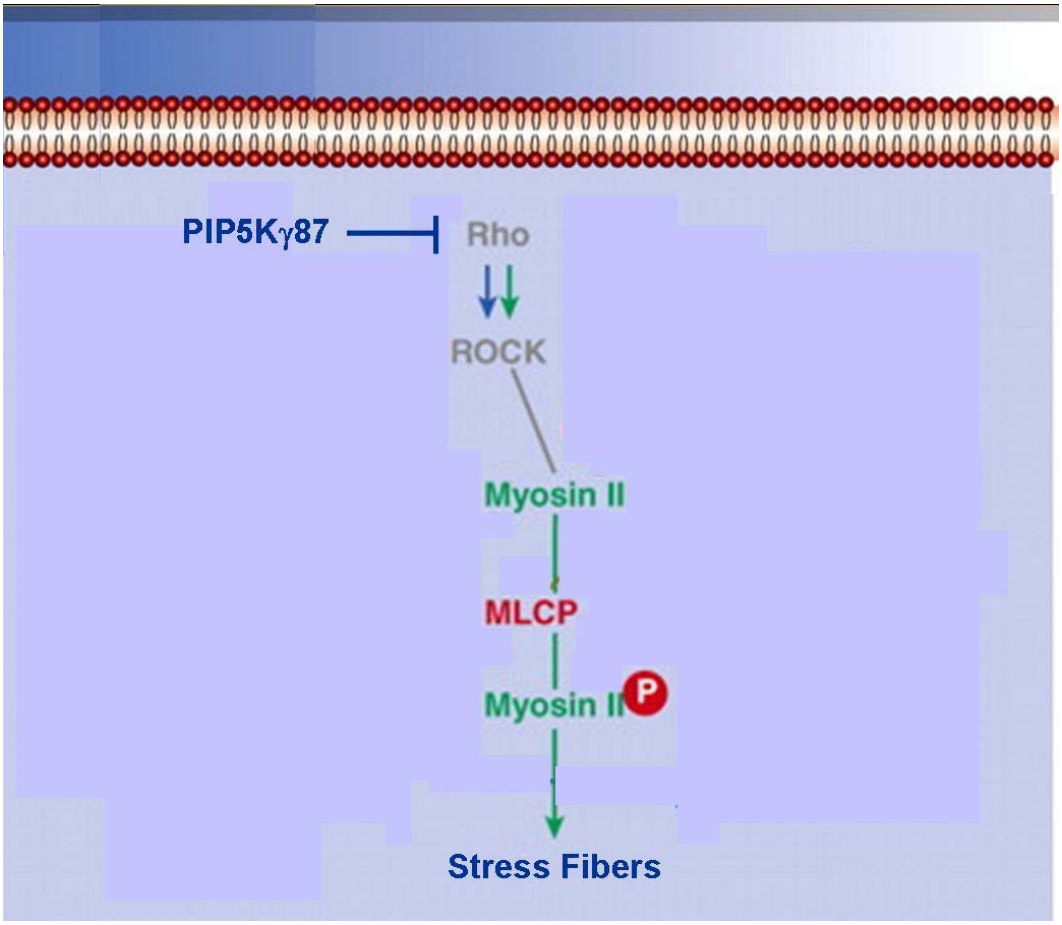
PIP5Kγ87
Rho
ROCK
Myosin II
MLCP
Myosin II
P
Stress Fibers

Figure 14. (Adapted, with permission, from Stossel et al., 2006.) RhoA regulates the activity of ROCK and ROCK activates myosin light chain and inhibits myosin phosphatase. We hypothesize that PIP5Kγ regulates the actin cytoskeleton by inhibiting RhoA, and thus, its downstream effectors ROCK and myosin.

BIBLIOGRAPHY

Aikawa, Y., and T.F.J. Martin. (2003) ARF6 regulates a plasma membrane pool of phosphatidylinositol(4,5)bisphosphate required for regulated exocytosis. *J. Cell Biol.* 162: 647-659.

Akiyama, C., N. Shinozaki-Narikawa, T. Kitazawa, T. Hamakubo, T. Kodama, and Y. Shibasaki. (2005) Phosphatidylinositol-4-phosphate 5-kinase γ is associated with cell-cell junction in A431 epithelial cells. *Cell Biol. Int.* 29: 514-520.

Amano, M., M. Ito, K. Kimura, Y. Fukata, K. Chihara, T. Nakano, Y. Matsuura, and K. Kaibuchi. (1996) Phosphorylation and activation of myosin by rho-associated kinase. *J. Biol. Chem.* 271: 20246-20249.

Arthur, W.T. and K. Burridge. (2001) RhoA inactivation by p190RhoGAP regulates cell spreading and migration by promoting membrane protrusion and polarity. *Mol. Biol. Cell.* 12: 2711-2720.

Bairstow, S.F., K. Ling, and R.A. Anderson. (2005) Phosphatidylinositol phosphate kinase type Iγ directly associates with and regulates Shp-1 tyrosine phosphatase. *J. Biol. Chem.* 280: 23884-23891.

Bairstow, S.F., K. Ling, X. Su, A.J. Firestone, C. Carbonara, and R.A. Anderson. (2006) Type 1γ661 phosphatidylinositol phosphate kinase directly interacts with AP2 and regulates endocytosis. *J. Biol. Chem.* 281: 20632-20642.

Bakolitsa, C., J.M. de Pereda, C.R. Bagshaw, D.R. Critchley, and R.C. Liddington. (1999) Crystal structure of the vinculin tail suggests a pathway for activation. *Cell*. 99: 603-613.

Bakolitsa, C., D.M. Cohen, L.A. Bankston, A.A. Bobkov, G.W. Cadwell, L. Jennings, D.R. Critchley, S.W. Craig, and R.C. Liddington. (2004) Structural basis for vinculin activation at sites of cell adhesion. *Nature*. 430: 583-586.

Borgon, R.A., C. Vonrhein, G. Bricogne, P.R.J. Boris, and T. Izard. (2004) Crystal structure of human vinculin. *Structure.* 12: 1189-1197.

Boronenkov, I.V., J.C. Loijens, M. Umeda, and R.A. Anderson. (1998) Phosphoinositide signaling pathways in nuclei are associated with nuclear speckles containg pre-mRNA processing factors. *Mol. Biol. Cell.* 9: 3547-3560.

Caswell, P. and J. Norman. (2008) Endocytic transport of integrins during cell migration and invasion. *Trends in Cell Biol.* 18: 257-263.

Chao, W. and J. Kunz. (2009) Focal adhesion disassembly requires clathrin-dependent endocytosis of integrins. *FEBS Letters.* 583: 1337-1343.

Chandrasekar, I., T.E.B. Stradal, M.R. Holt, F. Entschladen, B.M. Jockusch, and W.H. Ziegler. (2005) Vinculin acts as a sensor in lipid regulation of adhesion-site turnover. *J. Cell Sci.* 118: 1461-1472.

Chen, H., D.M. Cohen, D.M. Choudhury, N. Kioka, and S.W. Craig. (2005) Spatial distribution and functional significance of activated vinculin in living cells. *J. Cell Biol.* 169: 459-470.

Chen, M.Z., X. Zhu, H. Sun, Y.S. Mao, Y. Wei, M. Yamamoto, and H.L. Yin. (2009) Oxidative stress decreases phosphatidylinositol 4,5-bisphosphate levels by deactivating phosphatidylinositol-4-phosphate 5-kinase β in a syk-dependent manner. *J. Biol. Chem.* 284: 23743-23753.

Chong, L.D., A. Traynor-Kaplan, G.M. Bokoch, and M.A. Schwartz. (1994) The small GTP-binding protein Rho regulates a phosphatidylinositol 4-phosphate 5-kinase in mammalian cells. *Cell.* 79: 507-513.

Coll, J.L., A. Ben-Ze'ez, R.M Ezzell, J.L.R. Fernandez, H. Baribault, R.G. Oshima, and E.D. Adamson. (1995) Targeted disruption of vinculin genes in F9 and embryonic stem cells changes cell morphology, adhesion, and locomotion. *Proc. Natl. Acad. Sci. USA.* 92: 9161-9165.

Coppolino, M.G., R. Dierckman, J. Loijens, R.F. Collins, M. Pouladi, J. Jongstra-Bilen, A.D. Schreiber, W.S. Trimble, R. Anderson, and S. Grinstein. (2002) Inhibition of phosphatidylinositol-4-phosphate 5-kinase Iα impairs localized actin remodeling and suppresses phagocytosis. *J. Biol. Chem* 277: 43849-43857.

Corgan, A.M., C.A. Singleton, C.B. Santoso, and J.A. Greenwood. (2004) Phosphoinositides differentially regulate α-actinin flexibility and function. *Biochem. J.* 378: 1067-1072.

Cox, D., P. Chang, T. Kurosaki, and S. Greenberg. (1996) Syk tyrosine kinase is required for immunoreceptor tyrosine activation motif-dependent actin assembly. *J. Biol. Chem.* 271: 16597-16602.

Cox, E.A., S.K. Sastry, and A. Huttenlocher. (2001) Integrin-mediated adhesion regulates cell polarity and membrane protrusion through the Rho family of GTPases. *Mol. Biol. Cell.* 12: 265-277.

De Pereda, J.M., K.L. Wegener, E. Santelli, N. Bate, M.H. Ginsberg, D.R. Critchley, I.D. Campbell, and R.C. Liddington. (2005) Structural basis for phosphatidylinositol phosphate kinase type Iγ binding to talin at focal adhesions. *J. Cell Biol.* 280: 8381-8386.

Di Paolo, G., L. Pellegrini, K. Letinic, G. Cestra, R. Zoncu, S. Voronov, S. Chang, J. Guo, M.R. Wenk, and P. De Camilli. (2002) Recruitment and regulation of phosphatidylinositol phosphate kinase type 1γ by the FERM domain of talin. *Nature.* 420: 85-89.

Di Paolo, G., H.S. Moskowitz, K. Gipson, M.R. Wenk, S. Voronov, M. Obayashi, R. Flavell, R.M. Fitzsimonds, T.A. Ryan, and P. De Camilli. (2004) Impaired PtdIns(4,5)P_2 synthesis in nerve terminals produces defects in synaptic vesicle trafficking. *Nature*. 431: 415-422.

Divecha, N., M. Roefs, J.R. Halstead, S. D'Andrea, M. Fernandez-Borga, L. Oomen, K.M. Saqib, M.J.O. Wakelam, and C. D'Santos. (2000) Interaction of the type Iα PIPkinase with phospholipase D: a role for the local generation of phosphatidylinositol 4,5-bisphosphate in the regulation of PLD2 activity. *EMBO J.* 19: 5440-5449.

Doughman, R.L., A.J. Firestone, and R.A. Anderson. (2003a) Phosphatidylinositol phosphate kinases put PI4,5P_2 in its place. *J. Membr. Biol.* 194: 77-89.

Doughman, R.L., A.J. Firestone, M.L. Wojtasiak, M.W. Bunce, and R.A. Anderson. (2003b) Membrane ruffling requires coordination between type Iα phosphatidylinostitol phosphate kinase and rac signaling. *J. Biol. Chem.* 278: 23036-23045.

Dunphy, J.L., R. Moravec, K. ly, T.K. Lasell, P. Melancon, and J.E. Casanova. (2006) The Arf6 GEF GEP100/BRAG2 regulates cell adhesion by controlling endocytosis of β1 integrins. *Curr. Biol.* 16: 315-320.

Fernandez, J.L.R., B. Geiger, D. Salomon, and A. Ben-Ze'ev. (1992) Overexpression of vinculin suppresses cell motility in BALB/c 3T3 cells. *Cell Motil. Cytoskeleton.* 22: 127-134.

Fernandez, J.L.R., B. Geiger, D. Salomon, and A. Ben-Ze'ev. (1993) Suppression of vinculin expression by antisense transfection confers changes in cell morphology, motility, and anchorage-dependent growth of 3T3 cells. *J. Cell Biol.* 122: 1285-1294.

Fraley, T.S., T.C. Tran, A.M. Corgan, C.A. Nash, J. Hao, D.R. Critchley, and J.A. Greenwood. (2003) Phosphoinositide binding inhibits α-actinin bundling activity. *J. Biol. Chem.* 278: 24039-24045.

Fraley, T.S., C.B. Pereira, T.C. Tran, C.A. Singleton, and J.A. Greenwood. (2005) Phosphoinositide binding regulates α-actin dynamics mechanism for modulating cytoskeletal remodeling. *J. Biol. Chem.* 280: 15479-15482.

Fukami, K., N. Sawada, T. Endo, and T. Takenawa. (1996) Identification of a phosphatidylinositol 4,5-bisphosphate-binding site in chicken skeletal muscle α-actinin. *J. Biol. Chem.* 271: 2646-2650.

Gilmore, A.P. and K. Burridge. (1996) Regulation of vinculin binding to talin and actin by phosphatidyl-inositol-4-5-bisphosphate. *Nature.* 381: 531-535.

Giudici, M., P.C. Emson, and R.F. Irvine. (2004) A novel neuronal-specific splice variant of type I phosphatidylinositol 4-phosphate 5-kinase isoform γ. *Biochem. J.* 379: 489-496.

Goksoy, E., Y. Ma, X. Wang, X. Kong, D. Perera, E.F. Plow, and J. Qin. (2008) Structural basis for the autoinhibition of talin in regulating integrin activation. *Mol. Cell*. 31: 124-133.

Gupton, S.L. and C.M. Waterman-Storer. (2006) Spatiotemporal feedback between actomyosin and focal-adhesion system optimizes rapid cell migration. *Cell.* 125: 1361-1374.

Halstead, J.R., J. van Rheenen, M.H.J. Snel, S. Meeuws, S. Mohammed, C.S. D'Santos, A.J. Heck, K. Jalink, and N. Divecha. (2006) A role for PtdIns(4,5)P_2 in regulating stress-induced apoptosis. *Curr. Biol.* 16: 1850-1856.

Huttelmaier, S., O. Mayboroda, B. Harbeck, T. Jarchau, B.M. Jockusch, and M. Rudiger. (1998) The interaction of the cell-contact proteins VASP and vinculin is regulated by phosphatidylinositol-4,5-bisphosphate. *Curr. Biol.* 8: 479-488.

Hynes, R.O. and A.D. Lander. (1992) Contact and adhesive specificities in the associations, migrations, and targeting of cells and axons. *Cell*. 69: 303-322.

Hynes, R.O. (1999) Cell adhesion: old and new questions. *Trends Biochem. Sci.* 24: M33-M37.

Ishihara, H., Y. Shibasaki, N. Kizuki, H. Katagiri, Y. Yazaki, T. Asano, and Y. Oka. (1996) Cloning of cDNAs encoding two isoforms of 68-kDa type I phosphatidylinositol4-phosphate 5-kinase. *J. Biol. Chem.* 271: 23611-23614.

Ishihara, H., Y. Shibasaki, N. Kizuki, T. Wada, Y. Yazaki, T. Asano, and Y. Oka. (1998) Type I phosphatidylinositol-4-phosphate 5-kinases. *J. Biol. Chem.* 273: 8741-8748.

Ishizaki, T., M. Maekawa, K. Fujisawa, K. Okawa, A. Iwamatsu, A. Fujita, N. Watanabe, Y. Saito, A. Kakizuka, N. Morii, and S. Narumiya. (1996) The small GTP-binding protein Rho binds to and activates a 160 kDa Ser/Thr protein kinase homologous to myotonic dystrophy kinase. *EMBO J.* 15: 1885-1893.

Kimura, K. M. Ito, M. Amano, K. Chihara, Y. Fukata, M. Nakafuku, B. Yamamori, J. Feng, T. Nakano, K. Okawa, A. Iwamatsu, and K. Kaibuchi. (1996) Regulation of myosin phosphatase by rho and rho-associated kinase. *Science.* 273: 245-248.

Kisseleva, M., Y. Feng, M. Ward, C. Song, R.A. Anderson, and G.D. Longmore. (2005) The LIM protein ajuba regulates phosphatidylinostiol 4,5-bisphosphate levels in migrating cells through an interaction with and activation of PIP5KIα. *Mol. Cell Biol.* 25: 3956-3966.

Kong, X., X. Wang, S. Misra, and J. Qin. (2006) Structural basis for the phosphorylation-regulated focal adhesion targeting of type Iγ phosphatidylinositol phosphate kinase (PIPKIγ) by talin. *J. Mol. Biol.* 359: 47-54.

Kovacs, M., J. Toth, C. Hetenyi, A. Malnasi-Csizmadia, and J.R. Sellers. (2004) Mechanism of blebbistatin inhibition of myosin II. *J. Cell Biol.* 279: 35557-35563.

Krauss, M., M. Kinuta, M.R. Wenk, P. De Camilli, K. Takei, and V. Haucke. (2003) ARF6 stimulates clathrin/AP-2 recruitment to synaptic membranes by activating phosphatidylinositol phosphate kinase type Iγ. *J. Cell Biol.* 162: 113-124.

Krauss, M., V. kukhtina, A. Pechstein, and V. Haucke. (2006) Stimulation of phosphatidylinositol kinase type 1-mediated phosphatidylinositol (4,5)-bisphosphate synthesis by AP-2μ-cargo complexes. *Proc. Natl. Acad. Sci. USA.* 103: 11934-11939.

Kueng, W., E. Silber, and U. Eppenberger. (1989) Quantification of cells cultured on 96-well plates. *Anal. Biochem.* 182: 16-19.

Lee, S.Y., S. Voronov, K. Letinic, A.C. Nairn, G. Di Paolo, and P. De Camilli. (2005) Regulation of the interaction between PIP5KIγ and talin by proline-directed protein kinases. *J. Cell Biol.* 168: 789-799.

Leung, T. E. Manser, L. Tan, and L. Lim. (1995) A novel serine/threonine kinase binding the ras-related RhoA GTPase which translocates the kinase to peripheral membranes. *J. Biol. Chem.* 270: 29051-29054.

Li, J., B.A. Ballif, A.M. Powelka, J. Dai, S.P. Gygi, and V.W. Hsu. (2005) Phosphorylation of ACAP1 by Akt regulates the stimulation-dependent recycling of integrin β1 to control cell migration. *Dev. Cell.* 9: 663-673.

Liddington, R.C. and M.H. Ginsber. (2002) Integrin activation takes shape. *J. Cell Biol.* 158: 833-839.

Ling, K., R.L. Doughman, A.J. Firestone, M.W. Bunce, and R.A. Anderson. (2002) Type 1γ phosphatidylinositol phosphate kinase targets and regulates focal adhesions. *Nature.* 420: 89-93.

Ling, K., R.L. Doughman, V.V. Iyer, A.J. Firestone, S.F. Bairstow, D.V. Mosher, M.D. Schaller, and R.A. Anderson. (2003) Tyrosine phosphorylation of type 1γ phosphatidylinositol phosphate kinase by Src regulates an integrin-talin switch. *J. Cell Biol.* 163: 1339-1349.

Ling, K., S.F. Bairstow, C. Carbonara, D.A. Turbin, D.G. Huntsman, and R.A. Anderson. (2007) Type 1γ phosphatidylinositol phosphate kinase modulates

adherens junction and E-cadherin trafficking via a direct interaction with μ1B adaptin. *J. Cell Biol.* 176:343-363.

Loijens, J.C. and R.A. Anderson. (1996) Type I phosphatidylinositol-4-phosphate 5-kinases are distinct members of this novel lipid kinase family. *J. Cell Biol.* 271: 32937-32943.

Lokuta, M.A., M.A. Senetar, D.A. Bennin, P.A. Nuzzi, K.T. Chan, V.L. Ott, and A. Huttenlocher. (2007) Type 1γ PIP kinase is a novel uropod component that regulates rear retraction during neutrophil chemotaxis. *Mol. Biol. Cell*. 18: 5069-5080.

Mao, Y.S. and H.L. Yin. (2007) Regulation of the actin cytoskeleton by phosphatidylinositol 4-phosphate 5 kinase. *Eur. J. Physiology.* 455: 1432-2013.

Mao, Y.S., M. Yamaga, X. Zhu, Y. Wei, H. Sun, J. Wang, M. Yun, Y. Wang, G. Di Paolo, M. Bennett, I. Mellman, C.S. Abrams, P. De Camilli, C.Y. Lu, and H.L. Yin. (2009) *J. Cell Biol.* 184: 281-296.

Martel, V., C. Racaud-Sultan, S. Dupe, C. Marie, F. Paulhe, and A. Galmiche. (2001) Conformation, localization, and integrin binding of talin depends on its interaction with phosphoinositides. *J. Biol. Chem.* 276: 21217-21227

Matsui, T., M. Amano, T. Yamamoto, K. chihara, M. Nakafuku, M. Ito, T. Nakano, K. Okawa, A. Iwamuatsu, and K. Kaibuchi. (1996) Rho-associated kinase, a novel serine/threonine kinase, as a putative target for the small GTP binding protein Rho. *EMBO J.* 15: 2209-2216.

Monkley, S.J., C.A. Pritchard, and D.R. Critchley. (2001) Analysis of the mammalian talin2 gene TLN2. *Biochem. Biophys. Res. Commun.* 286: 880-885.

Morgan, J.R., G. Di Paolo, H. Werner, V.A. Shchedrina, M. Pypaert, V.A. Pieribone, and P. De Camilli. (2004) A role for talin in presynaptic function. *J. Cell Biol.* 167: 43-50.

Nakano-Kobayashi, A., M. Yamazaki, T. Unoki, T. Hongu, C. Murata, R. Taguchi, T. Katada, M.A. Frohman, T. Yokozeki, and Y. Kanaho. (2007) Role of activation of PIP5Kγ661 by AP-2 complex in synaptic vesicle endocytosis. *Embo J.* 26: 1105-1116.

Narkis, G., R. Ofir, D. Landau, E. Manor, M. Volokita, R. Hershkowitz, K. Elbedour, and O.S. Birk. (2007) Lethal contractural syndrom type 3 (LCCS3) is caused by a mutation in PIP5K1C, which encodes PIPK1γ of the phosphatidylinsitol pathway. *Am. J. Hum. Genet.* 81: 530-539.

Nelson, C.D., J.J. Kovacs, K.N. Nobles, E.J. Whalen, and R.J. Lefkowitz. (2008) β-arrestin scaffolding of phosphatidylinositol 4-phosphate 5-kinase Iα promotes agonist-stimulated sequestration of the β2-adrenergic receptor. *J. Biol. Chem*. 283: 21093-21101.

Otey, C.A., F.M. Pavalko, and K. Burridge. (1990) An Interaction between α-actinin and the β_1 integrin subunit in vitro. *J. Cell Biol.* 111: 721-729.

Oude Weernink, P.A., P. Schulte, Y. Guo, J. Wetzel, M. Amano, K. Kaibuchi, S. Haverland, M. Vob, M. Schmidt, G.W. Mayer, and K.H. Jakobs. (2000)

Stimulation of phosphatidylinositol-4-phosphate 5-kinase by rho kinase. *J. Biol. Chem.* 275: 10168-10174.

Oude Weernink, P.A., K. Meletiadis, S. Hommeltenberg, M. Hinz, H. Ishihara, M. Schmidt, and K.H. Jakobs. (2004) Activation of type I phosphatidylinositol 4-phosphate 5-kinase isofroms by the Rho GTPases RhoA, Rac1, and Cdc42. *J. Biol. Chem.* 279:7840-7849.

Padron, D., Y.J. Wang, M. Yamamoto, H. Yin, and MG. Roth. (2003) Phosphatidylinositol phosphate 5-kinase 1β recruits AP-2 to the plasma membrane and regulates rates of constitutive endocytosis. *J. Cell. Biol.* 162: 693-701.

Pavalko, F.M. and K. Burridge. (1991) Disruption of the actin cytoskeleton after microinjection of proteolytic fragments of α-actinin. *J. Cell Biol.* 114: 481-491.

Powelka, A.M., J. Sun, J. Li, M. Gao, L.M. Shaw, A. Sonnenberg, and V.W. Hsu. (2004) Stimulation-dependent recycling of integrin β1 regulated by ARF6 and Rab11. *Traffic.* 5: 20-36.

Powner, D.J., R.M. Payne, T.R. Pettitt, M.L. Giudici, R.F. Irvine, and M.J.O. Wakelam. (2005) Phospholipase D2 stimulates integrin-mediated adhesion via phosphatidylinositol 4-phosphate 5-kinase Iγb. *J. Cell Sci.* 118: 2975-2986.

Priddle, H., L. Hemmings, S. Monkley, A. Woods, B. Patel, D. Sutton, G.A. Dunn, D. Zicha, and D.R. Critchley. (1998) Disruption of the talin gene

compromises focal adhesion assembly in undifferentiated but not differentiated embryonic stem cells. *J. Cell Biol.* 142: 1121-1133.

Ren, X.D., G.M. Bokoch, A. Traynor-Kaplan, G.H. Jenkins, R.A. Anderson, and M.A. Schwartz. (1996) Physical association of the small GTPase Rho with a 68-kDa phosphatidylinositol 4-phosphate 5-kinase in Swiss 3T3 cells. *Mol. Biol. Cell.* 7: 435-442.

Ren, X.D., W.B. Kiosses, and M.A. Schwartz. (1999) Regulation of the small GTP-binding protein Rho by cell adhesion and the cytoskeleton. *EMBO J.* 18: 578-585.

Ridley, A.J. and A. Hall. (1992) The small GTP-binding protein Rho regulates the assembly of focal adhesions and actin stress fibers in response to growth-factors. *Cell.* 70: 389-399.

Rottner, K., A. Hall, and J.V. Small. (1999) Interplay between Rac and Rho in the control of substrate contact dynamics. *Curr. Biol.* 9: 640-648.

Rozelle, A.L., L.M. Machesky, M. Yamamoto, M.H.E. Driessens, R.H. Insall, M.G. Roth, K. Luby-Phelps, G. Marriott, A. Hall, and H.L. Yin. (2000) Phosphatidylinositol 4,5-bispohsphate induces actin-based movement of raft-enriched vesicles through WASP-Arp2/3. *Curr. Biol.* 10: 311-320.

Sasaki, J., T. Sasaki, M. Yamazaki, K. Matsuoka, C. Taya, H. Shitara, S. Takasuga, M. Nishio, K. Mizuno, T. Wada, H. Miyazaki, H. Watanabe, R. Iizuka, S. Kubo, S. Murata, T. Chiba, T. Maehama, K. Hamada, H. Kishimoto, M.A. Frohman, K. Tanaka, J.M. Penninger, H. Yonekawa, A. Suzuki, and Y. Kanaho.

(2005) Regulation of anaphylactic responses by phosphatidylinositol phosphate kinase type Iα. *J. Exp. Med.* 201: 859-870.

Saunders, R.M., M.R. Holt, L. Jennings, D.H. Sutton, I.L. Barsukov, A. Bobkov, R.C. Liddington, E.A. Adamson, G.A. Dunn, and D.R. Critchley. (2006) Role of vinculin in regulating focal adhesion turnover. *Eur. J. Biochem.* 85: 487-500.

Sayegh, T.Y., P.D. Arora, K. Ling, C. Laschinger, P.A. Janmey, R.A. Anderson, and C.A. McCulloch. (2007) Phosphatidylinositol-4,5 bisphosphate produced by PIP5Kγ regulates gelsolin, actin assembly and adhesion strength of N-cadherin junctions. *Mol. Biol. Cell.* 8: 3026-3038.

Schwartz, M.A., M.D. Schaller, and M.H. Ginsberg. (1995) Integrins: emerging paradigms of signal transduction. *Annu. Rev. Cell Dev. Biol.* 11: 549-599.

Sprague, C.R., T.S. Fraley, H.S. Jang, S. Lal, and J.A. Greenwood. (2008) Phosphoinositide binding to the substrate regulates susceptibility to proteolysis by calpain. *J. Biol. Chem.* 283: 9217-9223.

Stephens, L.R., K.T. Hughes, and R.F. Irvine. (1991) Pathway of phosphatidylinositol(3,4,5)-trisphosphate synthesis in activated neutrophils. *Nature*. 351: 33-39.

Stossel, T.P., G. Fenteany, and J.H. Hartwig. (2006) Cell surface actin remodeling. *J. Cell Sci.* 119: 3261-3264.

Straight, A.F., A. Cheung, J. Limouze, I. Chen, N.J. Westwood, J.R. Sellers, T.J. Mitchison. (2003) Dissecting temporal and spatial control of cytokinesis with a myosin II inhibitor. *Science.* 299: 1743-1747.

Sun, Y., K. Ling, M.P. Wagoner, and R.A. Anderson. (2007) Type 1γ phosphatidylinositol phosphate kinase is required for EGF-stimulated directional cell migration. *J. Cell Biol.* 178: 297-308.

Tadokoro, S., S.J. Shattil, K. Eto, V. Tai, R.C. Liddington, J.M. de Pereda, M.H. Ginsberg, and D.A. Calderwood. (2003) Talin bindin to integrin β tails: a final common step in integrin activation. *Science.* 302: 103-106.

Thieman, J.R., S.K. Mishra, K. Ling, B. Doray, R.A. Anderson, and L.M. Traub. (2009) Clathrin regulates the association of PIPKIγ661 with the AP-2 adaptor β2 appendage. *J. Biol. Chem.* 284: 11392-13939.

Tolias, K.F., L.C. Cantley, and C.L. Carpenter. (1995) Rho family GTPases bind to phosphoinositide kinases. *J. Biol. Chem.* 270: 17656-17659.

Uehata, M., T. Ishizaki, H. Satoh, T. Ono, T. Kawahara, T. Morishita, H. Tamakawa, K. Yamagami, J. Inui, M. Maekawa, and S. Narumiya. (1997) Calcium sensitization of smooth muscle mediated by a Rho-associated protein kinase in hypertension. *Nature.* 389: 990-994.

Vasudevan, L., A. Jeromin, L. Volpicelli-Daley, P. De Camilli, D. Holowka, and B. Baird. (2009) The β- and γ-isoforms of type I PIP5K regulate distinct stages of Ca^{2+} signaling in mast cells. *J. Cell Sci.* 122: 2567-2574.

Wang, Y., L. Lian, J.A. Golden, E.E. Morrisey, and C.S. Abrams. (2007) PIP5Kγ is required for cardiovascular and neuronal development. *Proc. Natl. Acad. Sci. USA.* 104: 11748-11753.

Wang, Y., R.I. Litvinov, X. Chen, T.L. Bach, L. Lian, B.G. Petrich, S.J. Monkley, D.R. Critchley, T. Sasaki, M.J. Birnbaum, J.W. Weisel, J. Hartwig, and C.S. Abrams. (2008a) Loss of PIP5KIγ, unlike other PIP5KI isoforms, impairs the integrity of the membrane cytoskeleton in murine megakaryocytes. *Journal of Clinical Investigation*. 118: 812-819.

Wang, Y., X. Chen, L. Lian, T. Tang, T.J. Stalker, T. Sasaki, L.F. Brass, J.K. Choi, J.H. Hartwig, and C.S. Abrams. (2008b) Loss of PIP5KIβ deomonstrates that PIP5KI isoform-specific PIP_2 synthesis is required for IP_3 formation. *Proc. Natl. Acad. Sci. USA.* 105: 14064-14069.

Wang, Y.J., W.H. Li, J. Wang, K. Xu, P. Dong, X. Luo, and H.L. Yin. (2004) Critical role of PIP5KIγ87 in $InsP_3$-mediated Ca^{2+} signaling. *J. Cell Biol.* 167: 1005-1010.

Webb, D.J., Donais, K., L.A. Whitmore, S.M. Thomas, C.E. Turner, J.T. Parsons, and A.F. Horwitz. (2004) FAK-Src signaling through paxillin, ERK and MLCK regulates adhesion disassembly. *Nature Cell Biol.* 6: 154-161.

Weekes, J., S.T. Barry, and D.R. Critchley. (1998) Acidic phospholipids inhibit the intramolecular association between the N- and C-terminal regions of vinculin,

exposing actin-binding and protein kinase C phosphorylation sites. *Biochem. J.* 314: 827-832.

Wegener, K.L., A.W. Partridge, J. Han, A.R. Pickford, R.C. Liddington, M.H. Ginsberg, and I.D. Campbell. (2007) Structural basis of integrin activation by talin. *Cell.* 128: 171-182.

Wei, Q. and R.S. Adelstein. (2002) Pitx2a expression alters actin-myosin cytoskeleton and migration of HeLa cells through Rho GTPase signaling. *Mol. Biol. Cell.* 13: 683-697.

Whiteford, C.C., C.A. Brearley, and E.T. Ulug. (1997) Phosphatidylinositol 3,5-bisphosphate defines a novel PI 3-kinase pathway in resting mouse fibroblasts. *Biochem. J.* 323: 597-601.

Winograd-Katz, S.E., S. Itzkovitz, Z. Kam, and B. Geiger. (2009) Multiparametric analysis of focal adhesion formation by RNAi-mediated gene knockdown. *J. Cell Biol.* 186: 423-436.

Xu, W., H. Baribault, and E.D. Adamson. (1998a) Vinculin knockout results in heart and brain defects during embryonic development. *Development*. 125: 327-337.

Xu, W., J.L. Coll, and E.D. Adamson. (1998b) Rescue of the mutant phenotype by reexpression of full-length vinculin in null F9 cells; effects on cell locomotion by domain deleted vinculin. *J. Cell. Sci.* 111: 1535-1544.

Yamada, K.M. and D.W. Kennedy. (1984) Dualistic nature of adhesive protein function: fibronectin and its biologically active peptide fragments can autoinhibit fibronectin function. *J. Cell Biol.* 99: 29-36.

Zaidel-Bar, R. S. Itzkovitz, A. Ma'ayan, R. Iyengar, and B. Geiger. (2007) Functional atlas of the integrin adhesome. *Nat. Cell Biol.* 9: 858-867.

Zhang, X., G. Jiang, Y. Cai, S.J. Monkley, D.R. Critchley, and M.P. Sheetz. (2008) Talin depletion reveals independence of initial cell spreading from integrin activation and traction. *Nat. Cell Biol.* 10: 1062-1068.